Programming the Supramolecular Helical Polymerization of Dendritic Dipeptides via the Stereochemical Information of the Dipeptide

Brad M. Rosen,[†] Mihai Peterca,[†,‡] Kentaro Morimitsu,[†] Andrés E. Dulcey,[†] Pawaret Leowanawat,[†] Ana-Maria Resmerita,[†] Mohammad R. Imam,[†] and Virgil Percec*,[†]

[†]Roy & Diana Vagelos Laboratories, Department of Chemistry, University of Pennsylvania, Philadelphia, Pennsylvania 19104-6323, United States

[‡]Department of Physics and Astronomy, University of Pennsylvania, Philadelphia, Pennsylvania 19104-6396, United States

S *Supporting Information*

ABSTRACT: Many natural biomacromolecules are homochiral and are built from constituents possessing identical handedness. The construction of synthetic molecules, macromolecules, and supramolecular structures with tailored stereochemical sequences can detail the relationship between chirality and function and provide insight into the process that leads to the selection of handedness and amplification of chirality. Dendritic dipeptides, previously reported from our laboratory, self-assemble into helical porous columns and serve as fundamental

mimics of natural porous helix-forming proteins and supramolecular polymers. Herein, the synthesis of all stereochemical permutations of a self-assembling dendritic dipeptide including homochiral, heterochiral, and differentially racemized variants is reported. A combination of CD/UV—vis spectroscopy in solution and in film, X-ray diffraction, and differential scanning calorimetry studies in solid state established the role of the stereochemistry of the dipeptide on the thermodynamics and mechanism of self-assembly. It was found that the highest degree of stereochemical purity, enantiopure homochiral dendritic dipeptides, exhibits the most thermodynamically favorable self-assembly process in solution corresponding to the greatest degree of helical order and intracolumnar crystallization in solid state. Reducing the stereochemical purity of the dendritic dipeptide through heterochirality or by partially or fully racemizing the dendritic dipeptide destructively interferes with the self-assembly process. All dendritic dipeptides were shown to coassemble into single columns regardless of their stereochemistry. Because these columns exhibit no deracemization, the thermodynamic advantage of enantiopurity and homochirality suggests a mechanism for stereochemical selection and chiral amplification.
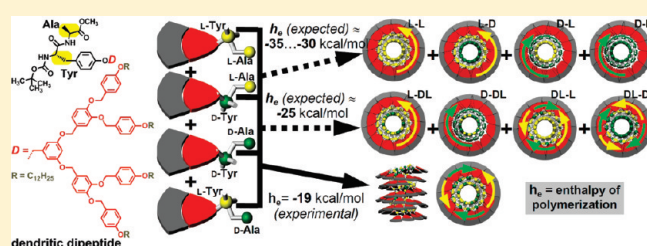
■ INTRODUCTION

Supramolecular polymers[1,2] are analogues of covalent polymers, wherein monomers are not linked by covalent bonds, but rather by the intermolecular interactions that define the realm of supramolecular chemistry.[3] Like covalent polymers, supramolecular polymers can be classified by their chemical structure and topology and by their mechanism of polymerization.[4−6] Supramolecular polymerization is facilitated by intermolecular interactions that mediate the connection between monomers, such as H-bonding,[7−12] $\pi-\pi$ and donor—acceptor interactions,[11−16] ionic interactions,[17] and host—guest interactions.[18] As delineated in a recent review by Meijer,[6] the thermodynamics of linear supramolecular polymerization can be either isodesmic or cooperative/anticooperative. In the isodesmic model,[19,20] the Gibbs free energy (ΔG) of monomer addition is independent of the degree of polymerization, whereas in the cooperative[13,21−23] or anticooperative supramolecular polymerization models the ΔG of monomer addition will increase or decrease following the formation of an oligomeric nucleus, respectively. Cooperativity can have a number of structural or environmental origins, but it is most frequently the result of helical growth triggered by the formation of a chiral nucleus. Helical cooperative growth is fundamental in biological self-assembly such as the supramolecular polymerization of proteins[21,24,25] and can be utilized to program biomimetic supramolecular polymerizations. Unlike many stereogenic synthetic polymers, which can be prepared as homochiral (e.g., isotactic), heterochiral (e.g., syndiotactic), or racemic (e.g., atactic), biopolymers such as proteins, polysaccharides, and nucleic acids exist almost exclusively in the homochiral form derived from enantiomerically pure building blocks. Therefore, it is difficult to probe the interrelationship of small numbers of stereocenters, their function, and the mechanism of chiral amplification that could result in the current level of stereopurity in nature. Fortuitously, synthetic systems have emerged that allow for the mimicry of the helical cooperative growth found in nature,[3] but with the flexibility to the relationship between fewer stereocenters.
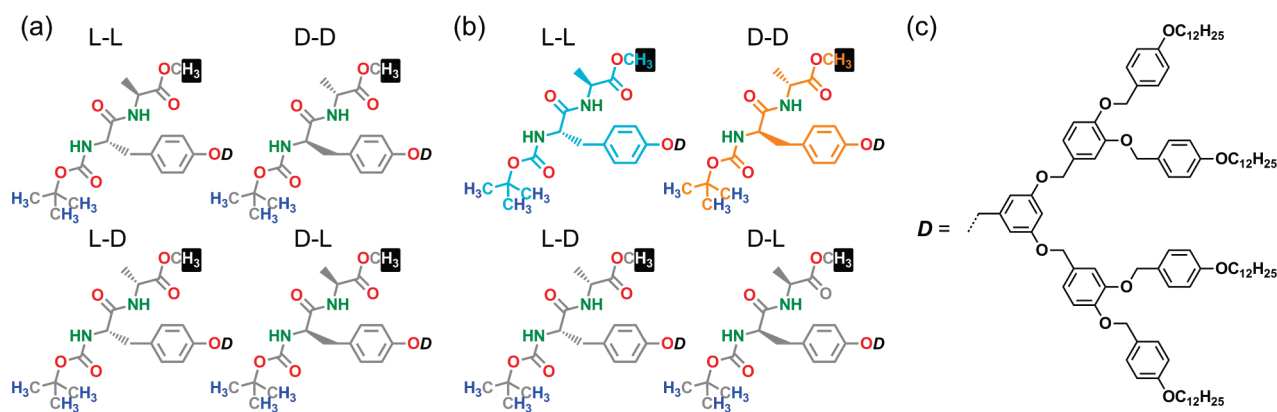
Figure 1. The structures of homochiral and heterochiral dendritic dipeptides (4-3,4-3,5)12G2-CH₂-Boc-X-Tyr-Y-Ala-OMe and the color code of the dipeptide used in the molecular models illustrating the cross-section of the porous columns. (a) Color code of L–L, D–D, L–D, and D–L dipeptides used for molecular models to illustrate the cross-sections of the supramolecular columns self-assembled from enantiopure homo- and heterochiral dendritic dipeptides ($-CH_3$ from the Boc group of Tyr, blue; $-CH_3$ of the methylester and methyl of Ala, white; C, gray; O, red; N–H, green). (b) Color code of L–L, D–D, L–D, and D–L dipeptides used to illustrate the cross-sections of the supramolecular columns self-assembled from the different racemic variants L–DL, D–DL, DL–L, DL–D, and DL–DL explained in Figure 2 ($-CH_3$ from Boc group of Tyr, blue; O, red; N–H, green; C in L–D and D–L, gray; C and $-CH_3$ groups of Ala in L–L and D–D, light blue and orange, respectively; $-CH_3$ groups of Ala in L–D and D–L, white). (c) Structure of the second generation dendron (4-3,4-3,5)12G2-.

Benzyl ether dendrons with specific primary structure functionalized with aliphatic or semifluorinated alkyl groups[2e,f,15b] self-assemble in solution and in solid state providing access to a multitude of periodic lattices and quasi-periodic arrays.[2g] They provide insight into the mechanism of self-assembly and access to the design of new self-organized structures.[26–29] Typical libraries utilized in the discovery process are comprised of mostly achiral dendrons.[26,30–32] The attachment of dipeptides to the apex of wedge-shaped self-assembling benzyl-ether dendrons[33a–d] induces asymmetry that is amplified through self-assembly into supramolecular helical porous columns that are stereochemically programmed and allosterically regulated.[8,33e] Similarly, the attachment of dipeptides to the apex of cone-shaped self-assembling dendrons provides hollow chiral spherical supramolecular dendrimers.[34] Adaptation of the Cochran, Crick, and Vand helical diffraction theory[35] to columnar supramolecular dendrimers demonstrated internal helical order generated from dendritic dipeptides in their supramolecular columns.[33b,36,37] The architecture of the internal structure of the supramolecular porous column and the self-assembly mechanism of dendritic dipeptides are of considerable interest in the design of related and unrelated complex functional systems such as self-repairing supramolecular electronic materials,[15,38] porous protein mimics,[33] supramolecular containers,[34] thixotropic gels,[39] and nanomechanical actuators.[40]

Herein, a single dendritic dipeptide with only two stereocenters, (4-3,4-3,5)12G2-CH₂-Boc-X-Tyr-Y-Ala-OMe, was prepared in all of its possible stereoisomeric forms, including homochiral, heterochiral, as well as singly and fully racemic combinations of α-amino acids. The study of the supramolecular polymerization of these stereoisomeric dendritic dipeptides in solution via CD/UV–vis spectroscopy and modeling of the helical cooperative growth process in tandem with differential scanning calorimetry (DSC) and X-ray diffraction (XRD) experiments in solid state established a helical cooperative growth mechanism and demonstrated how the stereochemical information of the dipeptide is amplified through the supramolecular polymerization process. Furthermore, it was shown how the
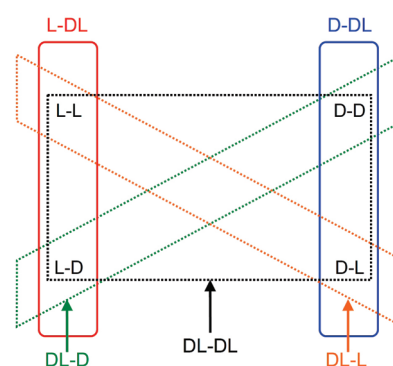

Figure 2. The enantiomeric composition of racemized dendritic dipeptides.

handedness of one stereocenter of the dipeptide can exhibit a preference for the same handedness in the second α-amino acid providing a mechanism for homochiral amplification. The amplification of homochirality can lead to increased intracolumnar order and to the emergence of function derived from chiral recognition and enhancement.

■ RESULTS AND DISCUSSION

Design and Synthesis of Dendritic Dipeptides. The dendron (4-3,4-3,5)12G2-X self-assembles in solution and self-organizes in the bulk state with a diversity of apex functionalities (X), including dipeptides.[33] When the dipeptide fragments are separated from the dendron sheath, they crystallize into an orthorhombic lattice derived from their inherent linear conformation.[33a] This is markedly different from their barrel-stave helical supramolecular structure of the dipeptide generated by the self-assembly of the dendritic dipeptide.[33a] Therefore, the self-assembly of the dendritic dipeptides (4-3,4-3,5)12G2-CH₂-Boc-X-Tyr-Y-Ala-OMe is driven by the dendron periphery and is sterochemically programmed by the dipeptide.[33e] To fully elaborate the relationship between the two stereocenters, the

Scheme 1. Synthesis of the New Dendritic Dipeptides (4-3,4-3,5)12G2-CH₂-Boc-Tyr-Ala-OMe[a]
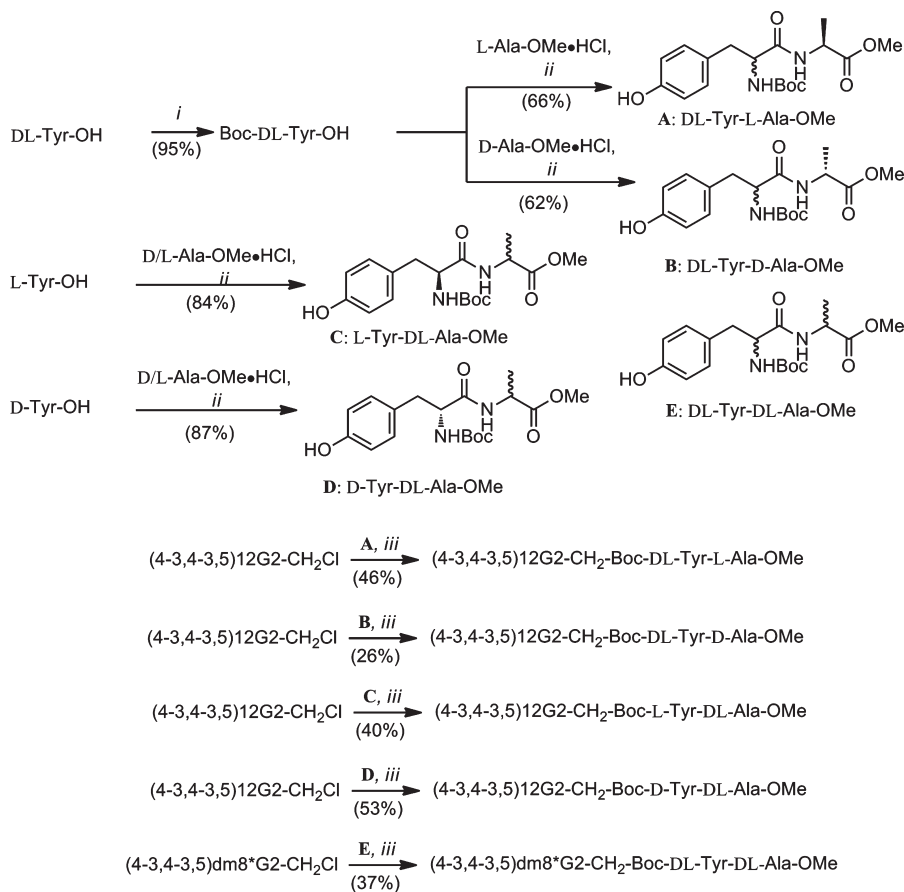
[a] Reagents and conditions: (i) di-*tert*-butyl dicarbonate, Et₃N, dioxane/H₂O, 0 °C, 24 h; (ii) NMM, CDMT, EtOAc, 2 h; (iii) K₂CO₃, DMF, 70 °C.

solution-phase supramolecular polymerization and solid-state self-organization of all four homochiral (L–L, D–D) and hetero-chiral (L–D, D–L) permutations of the dipeptide stereochemistry must be studied in depth (Figure 1).

Nevertheless, the synthesis and analysis of the four enantio-pure dendritic dipeptides does not address the mechanism of chiral amplification during self-assembly and self-organization. α-Amino acids can exist in either the dextrorotatory (D) or levorotatory form (L). Biologically synthesis of α-amino acids is highly enantioselective providing exclusively the L-form, while the D isomer can be prepared efficiently through asymmetric synthesis.[41] However, if one or both of the α-amino acids are not obtained through stereoselective synthesis and are subsequently coupled, a variety of partially and fully racemized dipeptides can be prepared (Figure 2). If Tyr is prepared in a racemic fashion and coupled to L-Ala, a 50:50 mixture of D-Tyr-L-Ala and L-Tyr-L-Ala will be obtained. This mixture is herein referred to as DL–L (Figure 2, orange parallelogram). Likewise, if Tyr is prepared in a racemic fashion and coupled to D-Ala, a 50:50 mixture of D-Tyr-D-Ala and L-Tyr-D-Ala will be generated. This mixture is referred to as DL–D (Figure 2, green parallelogram). If, on the other hand, Ala is prepared in racemic form and coupled with D-Tyr, a 50:50 mixture of D-Tyr-D-Ala and D-Tyr-L-Ala, D–DL, will be formed (Figure 2, blue rectangle). Conversely, when Ala is racemic and coupled with L-Tyr, a 50:50 mixture of L-Tyr-D-Ala and L-Tyr-L-Ala, L–DL, is accessed (Figure 2, red rectangle). Finally, if both Ala and Tyr are prepared racemic and coupled, a 25:25:25:25

mixture of D-Tyr-D-Ala, D-Tyr-L-Ala, L-Tyr-D-Ala, and L-Tyr-L-Ala, DL–DL, is obtained (Figure 2, red rectangle).

Ultimately, the Tyr–Ala dipeptides can be coupled to a dendron to form four stereoisomeric dendritic dipeptide variants, L–L, D–D, L–D, and D–L, obtained in nine different combinations that in addition to the four stereoisomers mentioned contain L–DL, D–DL, DL–L, DL–D, and DL–DL. For this study, five new partially or fully racemized dendritic dipeptides were synthesized: (4-3,4-3,5)12G2-CH₂-Boc-DL-Tyr-L-Ala-OMe, (4-3,4-3,5)12G2-CH₂-Boc-DL-Tyr-D-Ala-OMe, (4-3,4-3,5)12G2-CH₂-Boc-L-Tyr-DL-Ala-OMe, (4-3,4-3,5)12G2-CH₂-Boc-D-Tyr-DL-Ala-OMe, and (4-3,4-3,5)dm8*G2-CH₂-Boc-DL-Tyr-DL-Ala-OMe (Scheme 1). The previously reported homochiral and heterochiral benzyl ether[33a,e] and naphtyl ether[33g] dendritic dipeptides were synthesized according to previously reported procedures. Boc-DL-Tyr-OH was prepared in 95% by treating DL-Tyr-OH with di-*tert*-butyl dicarbonate and Et₃N in a 50/50 mixture of dioxane and H₂O. Nonracemic dipeptides were prepared in 62−87% yield via 2-chloro-4,6-dimethoxy-1,3,5-triazine (CDMT)[42]-mediated coupling of Boc-DL-Tyr-OH, Boc-L-Tyr-OH, or Boc-D-Tyr-OH with L-Ala-OMe·HCl, D-Ala-OMe·HCl, or DL-Ala-OMe·HCl respectively. Etherification of (4-3,4-3,5)12G2-CH₂Cl with the partially racemized dipeptides in DMF using K₂CO₃ as base provided the dendritic dipeptides (4-3,4-3,5)12G2-CH₂-Boc-DL-Tyr-L-Ala-OMe, (4-3,4-3,5)12G2-CH₂-Boc-DL-Tyr-D-Ala-OMe, (4-3,4-3,5)12G2-CH₂-Boc-L-Tyr-DL-Ala-OMe, and (4-3,4-3,5)12G2-CH₂-Boc-D-Tyr-DL-Ala-OMe in 26−53%

Scheme 2. Synthesis of the New Dendritic Dipeptides (6 Np-3,4-3,5)12G2-CH$_2$-Boc-Tyr-Ala-OMe and (6 Np-3,4-3,5)dm8*G2-CH$_2$-Boc-Tyr-Ala-OMe[a]
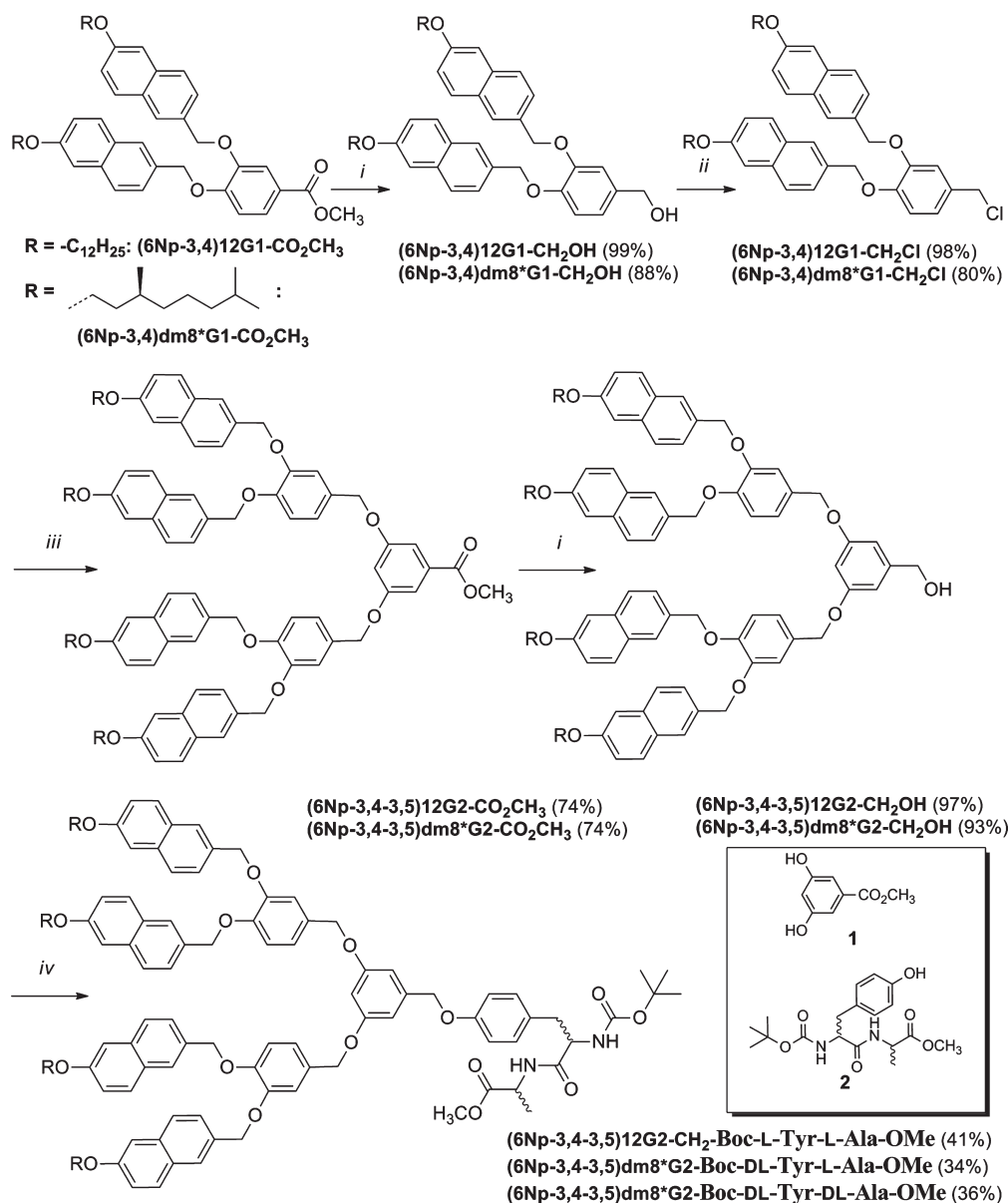
^{a} Reagents and conditions: (i) LiAlH$_4$, THF, 0 °C to room temperature; (ii) SOCl$_2$, DTBMP, 0 °C to room temperature; (iii) **1**, K$_2$CO$_3$, DMF, 80 °C; (iv) **2**, PPh$_3$, DIAD, THF, room temperature.

yield, respectively. Alternatively, etherification of (4-3,4-3,5)dm8*G2-CH$_2$Cl with the fully racemized dipeptide in DMF using K$_2$CO$_3$ as base provided (4-3,4-3,5)dm8*G2-CH$_2$-Boc-DL-Tyr-DL-Ala-OMe in 37%.

Finally, (6 Np-3,4-3,5)dm8*G2-CH$_2$OH and (6 Np-3,4-3,5)dm8*G2-CH$_2$Cl were prepared through an analogous method (Scheme 2). The syntheses of the (6 Np-3,4)12G1CH$_2$-CO$_2$CH$_3$ and (6 Np-3,4)dm8*G1CH$_2$-CO$_2$CH$_3$ intermediates were described previously.[43] The first generation dendrons were reduced to their corresponding alcohols with LiAlH$_4$. Treatment with SOCl$_2$ provided the generation one dendritic chlorides, which were alkylated onto methyl 3,5-dihydroxybenzoate in the presence of K$_2$CO$_3$ as base to yield (6 Np-3,4-3,5)12G2-CO$_2$CH$_3$ (74%) and (6 Np-3,4-3,5)dm8*G2-CO$_2$CH$_3$ (74%).

After reduction to the second generation alcohols, the (6 Np-3,4-3,5)12G2-CH$_2$OH and (6 Np-3,4-3,5)dm8*G2-CH$_2$OH were etherified with either Boc-L-Tyr-L-Ala-OMe, Boc-DL-Tyr-L-Ala-OMe, or Boc-DL-Tyr-DL-Ala-OMe under Mitsunobu conditions to provide the dendritic dipeptides (6 Np-3,4-3,5)12G2-CH$_2$-Boc-L-Tyr-L-Ala-OMe, (6 Np-3,4-3,5)dm8*G2-CH$_2$-Boc-DL-Tyr-L-Ala-OMe, and (4 Np-3,4-3,5)dm8*G2-CH$_2$-Boc-DL-Tyr-DL-Ala-OMe in 41%, 34%, and 36% yield, respectively. Detailed synthesis and analysis is available in the Supporting Information.

Homochiral versus Heterochiral Dendritic Dipeptides. Homochiral dendritic dipeptides are defined as having identical stereochemistry for both α-amino acids. They are (4-3,4-3,5)12G2-CH$_2$-Boc-D-Tyr-D-Ala-OMe (D–D) and (4-3,4-3,5)12G2-CH$_2$-Boc-L-Tyr-L-Ala-OMe (L–L).[33a] Heterochiral dendritic dipeptides are

5138

dx.doi.org/10.1021/ja200280h |J. Am. Chem. Soc. 2011, 133, 5135–5151

defined as having opposing stereochemistry for the two α-amino acids. In this case, they are (4-3,4-3,5)12G2-CH₂-Boc-D-Tyr-L-Ala-OMe (D–L) and (4-3,4-3,5)12G2-CH₂-Boc-L-Tyr-D-Ala-OMe (L–D). The two homochiral dendritic dipeptides are enantiomers of each other, as are the two heterochiral dendritic dipeptides,
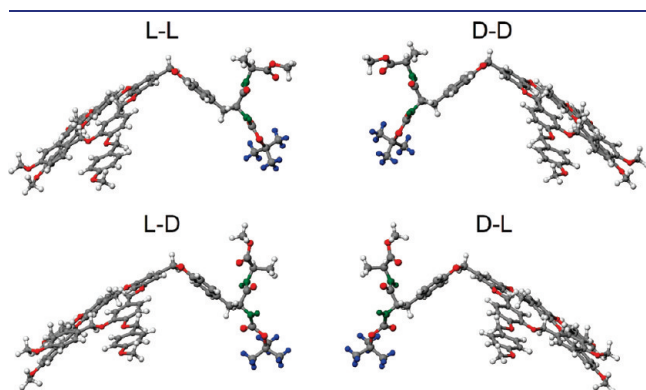
whereas the sets of homochiral and heterochiral dipeptides are diasteromers. The stereochemical relationships of the dendritic dipeptides manifest themselves structurally through enantiomeric and diastereomeric conformations (Figure 3). These conformations were determined via structural and retrostructural analysis of the self-organized dendritic dipeptides.[33] Helical diffraction theory was used to elucidate the spatial disposition of the dendritic dipeptides that give rise to the features observed in the oriented fiber X-ray diffraction pattern.[36] These structures are markedly different from the lowest energy conformations observed for the individual dendritic dipeptides.

The self-assembly of homochiral and heterochiral dendritic dipeptides can be analyzed both in solid state and in solution. In the solid state, both homochiral and heterochiral dendritic dipeptides self-assemble into helical porous columns that self-organize into hexagonal columnar lattices, Φ_h. The pore dimensions of homochiral dendritic dipeptides (D_{pore}) have been found to be slightly smaller than those observed for heterochiral dendritic dipeptides (Figure 4).[33a,e] A similar self-assembly process occurs in solution (1.6×10^{-4} M in cyclohexane). CD–UV–vis spectroscopy (Figure 5a–d) indicates that the sign of the Cotton effect and, therefore, the handedness of the supramolecular helix are determined by the stereochemistry of the Tyr residue and that the structural features of the columns are regulated by the stereochemistry of the Ala residue. The
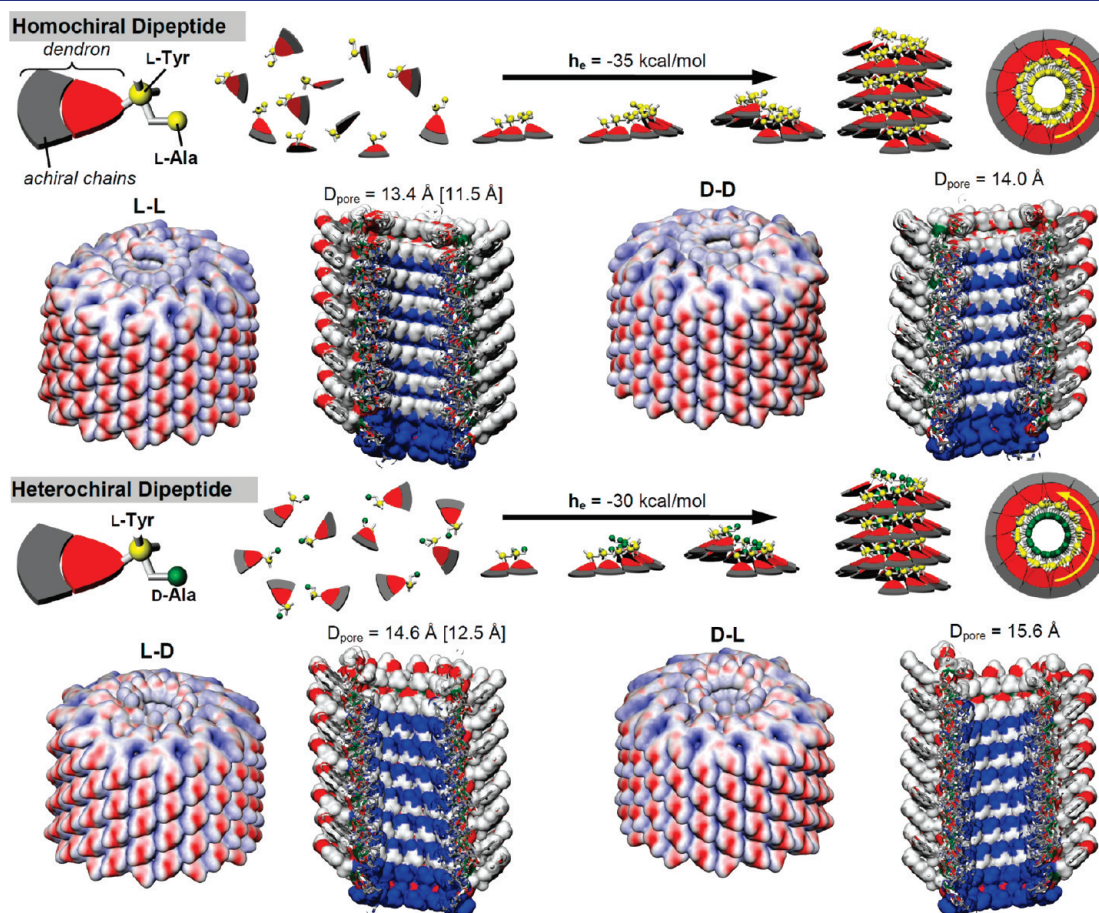

Figure 3. Molecular models of the four enantiopure dendritic dipeptides (4-3,4-3,5)12G2-CH₂-Boc-X-Tyr-Y-Ala-OMe obtained from the structural and retrostructural analysis of their supramolecular porous columns. For clarity and simplicity, their −C₁₂H₂₅ alkyl tails are represented by −CH₃.

Figure 4. Self-assembly of homochiral (top) and heterochiral (bottom) dendritic dipeptides in porous supramolecular columns via a helical cooperative growth. Schematic and analysis of self-assembly via supramolecular polymerization in solution and the corresponding side-view and cross-section of the porous supramolecular columns determined from XRD analysis in solid state. The color code of the dipeptides used in the cross-section of the supramolecular porous column is explained in Figure 1a.
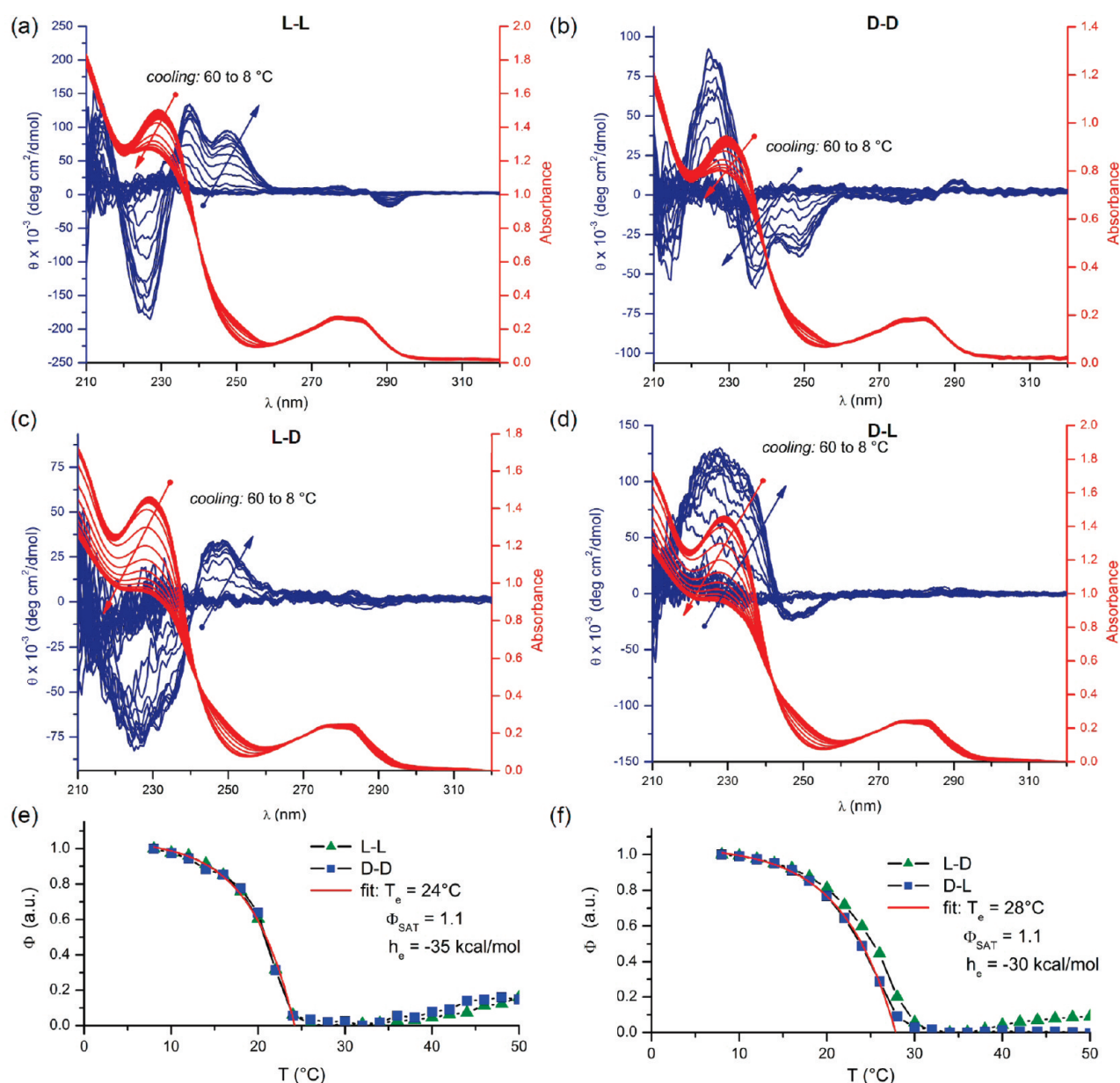
Figure 5. CD (blue) and UV−vis (red) of homochiral (a,b) and heterochiral (c,d) dendritic dipeptides (1.6×10^{-4} M in cyclohexane). Degree of aggregation as a function of temperature for homochiral (e) and heterochiral (f) dendritic dipeptides calculated from UV−vis spectra.

dominance of the Tyr stereochemistry is attributed to its direct connection to the dendritic periphery, through the phenolic residue. The self-assembled columnar structures found in the solid state have been demonstrated to be largely analogous to those in solution because the structures of homochiral and heterochiral dendritic dipeptides were found to be persistent in both states according to solution and thin film CD/UV−vis spectroscopy.[33a]

The self-assembly of dendritic dipeptides in solution is a form of supramolecular polymerization assisted by cooperative helical growth.[4] Like the Tobacco Mosaic Virus (TMV)[24] capsid proteins that served as a biological inspiration for self-assembling supramolecular dendrimers,[2f,44] the dendritic dipeptides are expected to nucleate into short single turns of the helix (e.g., lock-washer) followed by elongation or growth by addition of further dendritic dipeptides and/or by the stacking of already nucleated

lock-washer.[24,25,45] The thermodynamics of this supramolecular polymerization can be extracted and modeled by the methods described by Meijer[46−49] and van der Schoot.[23,50−52] In this approach, peak intensity maxima were selected from UV−vis spectra. Typically, peaks in the UV−vis spectra at about 230 nm were chosen for these experiments, and both heating and cooling cycles were investigated. At equivalent temperature and concentration, the ellipticities of the CD spectra of enantiomeric dendritic dipeptides do not always exhibit the same magnitude for identical enantiomeric purity. This is because the CD signal measured from self-assembled dendritic dipeptides is sensitive not only to the degree of aggregation but also to the kinetics of formation of helical order in the column. For this reason, the thermodynamics of supramolecular polymerization was determined from the UV−vis absorbance intensity profile, which is less sensitive to the perfection of the helical structure. The UV
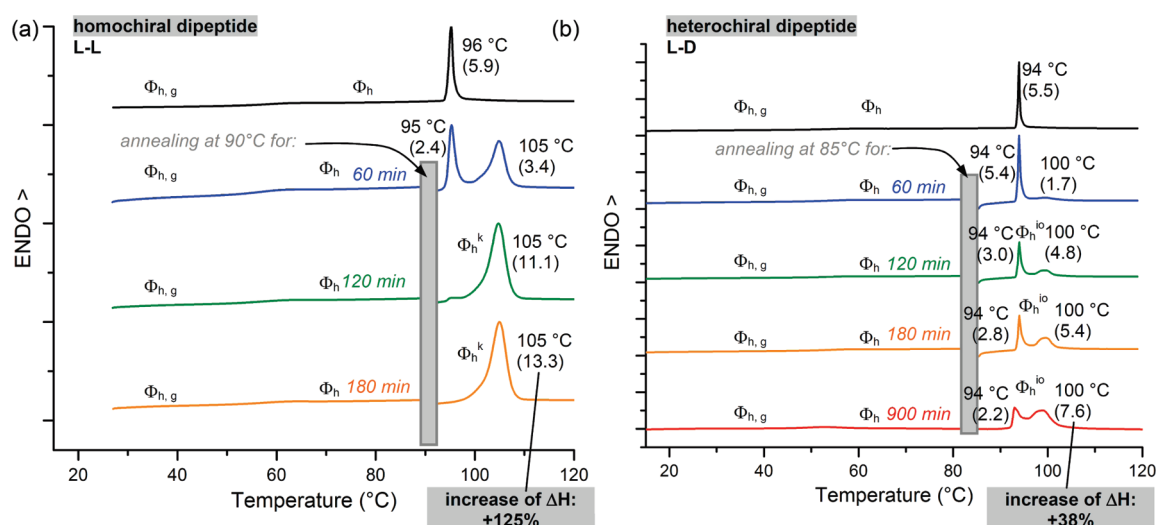
Figure 6. DSC traces upon heating of homochiral (L–L) (a) and heterochiral (L–D) (b) (4-3,4-3,5)12G2-CH₂-Boc-X-Tyr-Y-Ala-OMe with various annealing times prior to isotropization. The associated enthalpy changes are indicated in parentheses (kcal/mol).

Table 1. Thermal Transitions and Enthalpy Changes of Supramolecular Structures Assembled from Dendritic Dipeptides

dendron	dipeptide stereochemistry X—Y =	$t_{annealing}$ (min)	thermal transitions (°C) and corresponding enthalpy changes (kcal/mol) for the 10 °C/min heating DSC experiments without and with annealing
(4-3,4-3,5)12G2-	L–L, D–D	0	$\Phi_{h,g}$ 59 Φ_h 96 (5.9) i
		180	$\Phi_{h,g}$ 59 —annealing at 95 °C— Φ_h^k 105 (13.3) i
(4-3,4-3,5)12G2-	L–D, D–L	0	$\Phi_{h,g}$ 56 Φ_h 94 (5.5) i
		180	$\Phi_{h,g}$ 56 —annealing at 85 °C— Φ_h^{io} 100 (5.4) i
		900	$\Phi_{h,g}$ 56 —annealing at 85 °C— Φ_h^{io} 100 (7.6) i
(4-3,4-3,5)12G2-	L–DL, D–DL	0	$\Phi_{h,g}$ 55 Φ_h 94 (5.3) i
		180	$\Phi_{h,g}$ 55 —annealing at 80 °C— Φ_h 94 (5.6) i
(4-3,4-3,5)12G2-	DL–L, DL–D	0	$\Phi_{h,g}$ 55 Φ_h 94 (5.9) i
		180	$\Phi_{h,g}$ 55 —annealing at 80 °C— Φ_h 94 (6.1) i
(4-3,4-3,5)12G2-	DL–DL	0	$\Phi_{h,g}$ 55 Φ_h 93 (5.4) i
		180	$\Phi_{h,g}$ 55 —annealing at 80 °C— Φ_h 93 (5.9) i
(4-3,4-3,5)dm8*G2-	DL–DL	0	$\Phi_{h,g}$ 45 Φ_h 62 (3.5) i
(6 Np-3,4—3,5)dm8*G2-	DL–L	0	$\Phi_{h,g}$ 60 Φ_h 116 (4.8) i
(6 Np-3,4-3,5)dm8*G2-	DL–DL	0	$\Phi_{h,g}$ 60 Φ_h 116 (4.8) i
		180	$\Phi_{h,g}$ 61 —annealing at 100 °C— Φ_h 116 (4.8) i

absorbances for these peaks were rescaled such that 1.0 corresponds to the low temperature maximum or minimum intensity (i.e., maximum aggregation in the temperature range explored) and 0 corresponds to the high temperature maximum or minimum peak intensity (i.e., the molecularly dissolved species). For non-nucleated, isodesmic models of supramolecular polymerization, a sigmoidal relationship between the degree of aggregation and the temperature would have to be observed, whereas in a nucleated or cooperative helical growth model, a nonsigmoidal relationship between the degree of aggregation and temperature is expected.[51,52] Thermodynamic data can be obtained by fitting with the equation for the elongation domain according to Meijer (eq 1),[51b] where h_e is the molar enthalpy for polymerization, and T_e is the elongation temperature, or the point at which nucleation changes into elongation. For the cooperative helical growth model, T_e can be viewed as the temperature at which a complete turn of the helix

is formed allowing for enhanced h_e through structural reinforcement from the chiral nucleus.

$$\Phi = \Phi_{SAT}\left(1 - e^{[(-h_e/RT_e^2)(T - T_e)]}\right) \quad (1)$$

This thermodynamic analysis was applied to the supramolecular polymerization of homochiral and heterochiral dendritic dipeptides (4-3,4-3,5)12G2-CH₂-Boc-D-Tyr-D-Ala-OMe, (4-3,4-3,5)12G2-CH₂-Boc-L-Tyr-L-Ala-OMe, (4-3,4-3,5)12G2-CH₂-Boc-D-Tyr-L-Ala-OMe, and (4-3,4-3,5)12G2-Boc-L-Tyr-D-Ala-OMe (Figure 5e,f).

As expected, enantiomeric pairs (4-3,4-3,5)12G2-CH₂-Boc-D-Tyr-D-Ala-OMe/(4-3,4-3,5)12G2-CH₂-Boc-L-Tyr-L-Ala-OMe and (4-3,4-3,5)12G2-CH₂-Boc-D-Tyr-L-Ala-OMe/(4-3,4-3,5)12G2-CH₂-Boc-L-Tyr-D-Ala-OMe exhibit nearly identical self-assembly profiles. By fitting these profiles with the model for helical cooperative growth, it was found that the homochiral dendritic dipeptides transition from nucleation to elongation at 24 °C and exhibit a molar enthalpy of
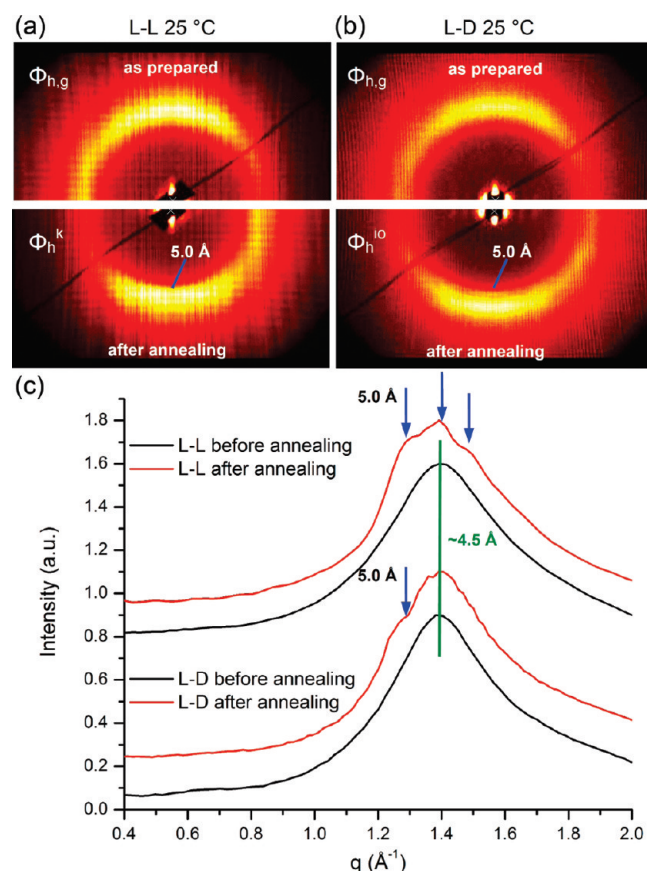
Figure 7. Wide-angle XRD patterns collected from the oriented fibers of the dendritic dipeptide (4-3,4-3,5)12G2-CH$_2$-Boc-X-Tyr-Y-AlaOMe, where X and Y are indicated (a). Meridional plots of the corresponding XRD patterns from (a) and (b) indicating that after annealing the homochiral dendritic dipeptide (L–L) changes from $\Phi_{h,g}$ into a Φ_h^k phase, and the heterochiral dendritic dipeptide (L–D) changes from $\Phi_{h,g}$ into a Φ_h^{io} phase (c).

monomer addition of −35 kcal/mol. On the other hand, heterochiral dendritic dipeptides are found to transition from nucleation to elongation at higher temperature 28 °C, but exhibit a lower molar enthalpy of monomer addition, −30 kcal/mol. While both homochiral and heterochiral dendritic dipeptides clearly exhibit helical cooperative growth during solution-phase supramolecular polymerization, these results indicate a more pronounced nucleation step for the homochiral dendritic dipeptides, which provides a more enthalpically favorable elongation process.

Self-assembly and self-organization of the dendritic dipeptides in the solid state can be viewed as a process analogous to their solution-phase supramolecular polymerization. However, higher effective monomer concentration and the effect of neighbor-to-neighbor column interactions result in a rapid nucleation and polymerization process at significantly elevated temperature (94−96 °C), taking the form of a first-order phase transition from the isotropic state (Figure 6). For the homochiral dendritic dipeptides, the transition ($T_{\Phi–I}$) from the hexagonal columnar phase (Φ_h) to the isotropic phase (I) occurs at 96 °C with a corresponding enthalpy of 5.9 kcal/mol (Figure 6a and Table 1). For the heterochiral dendritic dipeptide, $T_{\Phi–I}$ occurs at 94 °C with a lower corresponding enthalpy of 5.5 kcal/mol (Figure 6b and Table 1). Both homochiral and heterochiral dendritic dipeptides undergo a glass transition followed by the $\Phi_{h,g}$ phase

at lower temperature. To simulate the self-assembly process in the bulk state, the homochiral and heterochiral dendritic dipeptides were annealed just below $T_{\Phi–I}$ for 60, 120, 180, and 900 min (Figure 6). For both homochiral and heterochiral dendritic dipeptides, annealing resulted in the appearance of a second endothermic peak at higher temperature, which becomes more pronounced with increased annealing time. For the homochiral dendritic dipeptide, annealing for 120 or 180 min provided a complete shift in the isotropization by +9 °C and an increase in the enthalpy change associated with the first-order transition from ordered state to isotropic melt of 125%. These increases correspond to an intra- and intercolumnar crystallization process. However, for the heterochiral dendritic dipeptide, both transitions were still evident, even after 900 min of annealing. In this case, the new isotropization temperature is shifted by +6 °C and is accompanied by only a 38% increase in the enthalpy change associated with the first-order transition from the ordered to melt state.

The increased isotropization temperature and enthalpy change following the annealing of homochiral and heterochiral dendritic dipeptides is associated with changes to the order of the self-organized structures. WAXS performed on the oriented fibers indicate a slow transformation from a Φ_h phase to an ordered Φ_h^k phase following annealing of the homochiral dendritic dipeptide, as evidenced by significant amplification of 5.0 Å registry features[33b] relative to the short-range order diffuse broad peak at 4.5 Å (Figure 7a,c). In contrast, the WAXS fiber pattern collected after annealing from the heterochiral dendritic dipeptide exhibits the 5.0 Å registry features,[33b] but lacks the additional wide angle features of the Φ_h^k phase corresponding to intra- and intercolumnar long-range order, as indicated by the blue arrows in Figure 7c. In excellent agreement with the enthalphy changes calculated in Table 1, the XRD experiments revealed that the chirality of the second α-amino acid plays an important role in the formation of an ordered columnar phase or an intracolumnar ordered phase for the homochiral and heterochiral dendritic dipeptides, respectively. Furthermore, the combined XRD and DSC annealing experiments revealed that the intracolumnar crystallization, observed in both structures, is significantly faster in the case of homochiral structures.

Dendritic Dipeptides with One Racemized α-Amino Acid. Four dendritic dipeptides were prepared wherein one of their α-amino acids, Tyr or Ala, was racemic: (4-3,4-3,5)12G2-CH$_2$-Boc-DL-Tyr-D-Ala-OMe, (4-3,4-3,5)12G2-CH$_2$-Boc-DL-Tyr-L-Ala-OMe, (4-3,4-3,5)12G2-CH$_2$-Boc-D-Tyr-DL-Ala-OMe, and (4-3,4-3,5)12G2-CH$_2$-Boc-L-Tyr-DL-Ala-OMe. As described in Figure 2, each of these racemized structures represents a 50:50 mixture of diastereomeric homochiral and heterochiral dendritic dipeptides. The racemization of a single stereocenter of the dendritic dipeptide can affect the supramolecular expression of chirality, but could also significantly impact the mechanism of self-assembly. As a dendritic dipeptide racemized at one amino acid is comprised of a 50:50 mixture of diastereomeric dendritic dipeptides, the supramolecular polymerization can proceed through the incorporation of both dendrons into a single column or into two distinct columns, one corresponding to the homochiral dipeptide and the other corresponding to the heterochiral dipeptide (Figure 8).

CD−UV−vis spectroscopy analysis of dendritic dipeptides comprised of one racemic amino acid (Figure 9a−d) reveals that a single enantiopure Tyr residue maintains an overall net ellipticity with a sign determined by the handedness of the
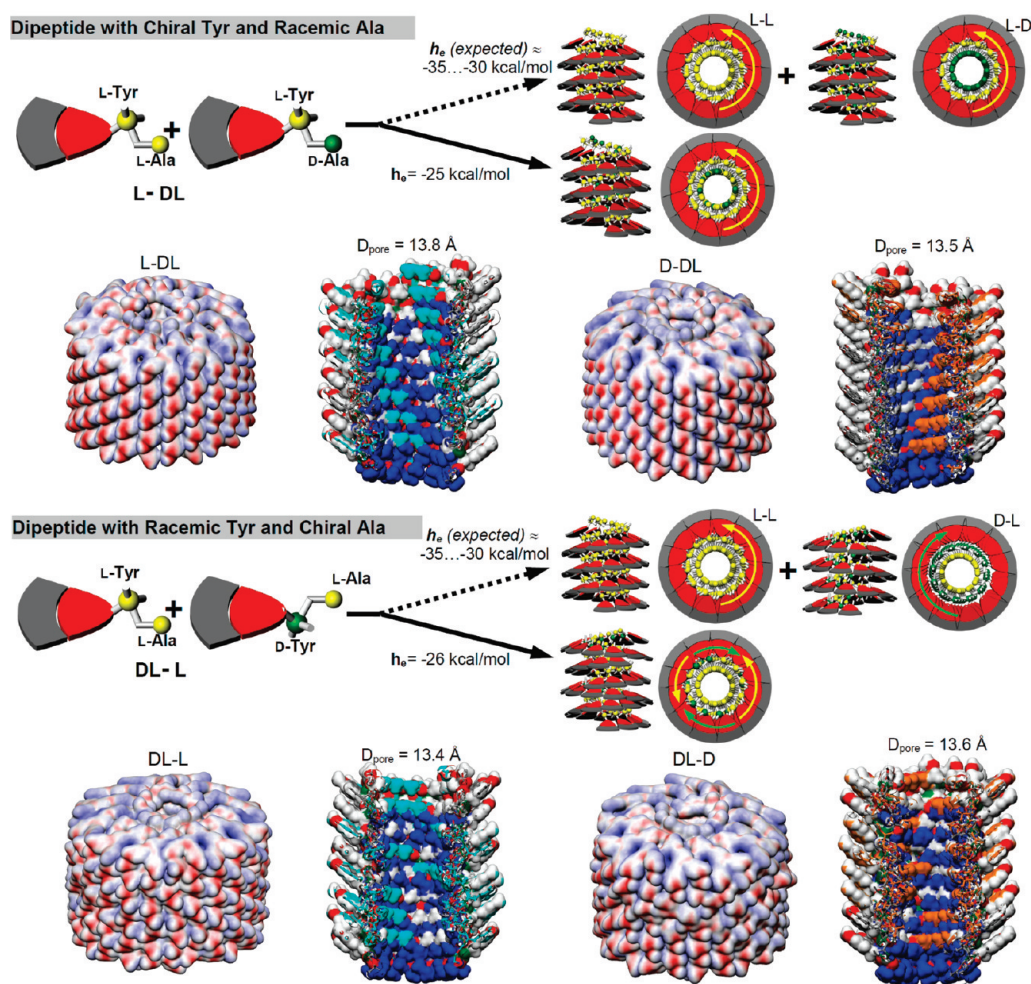
Figure 8. Self-assembly of dendritic dipeptides where Ala (top) or Tyr (bottom) has been racemized into porous supramolecular columns via a helical cooperative growth. Schematic and analysis of self-assembly via supramolecular polymerization in solution and the corresponding side-view and cross-section of the porous columns determined from XRD analysis in solid state. The color code of the dipeptides used in the cross-section of the porous supramolecular columns is explained in Figure 1b.

Tyr. On the other hand, a single enantiopure Ala residue in the conjunction with racemized Tyr provides no net ellipticity. If self-assembly of these singly racemized dendritic dipeptides occurs through two distinct columns composed of either homochiral or heterochiral dendritic dipeptides, we would expect both the temperature of the transition from nucleation to elongation and the molar enthalpy of monomer addition to be an average of what was observed for the homochiral and heterochiral columns, or $T_e = 26$ °C and $h_e = -32.5$ kcal/mol (Figure 8). Contrary to this expectation, for dendritic dipeptides composed of enantiopure Ala and racemized Tyr, (4-3,4-3,5)12G2-CH$_2$-Boc-D-Tyr-DL-Ala-OMe and (4-3,4-3,5)12G2-CH$_2$-Boc-L-Tyr-DL-Ala-OMe, a T_e of 21 °C and an h_e of 25 kcal/mol were observed (Figure 9e). Likewise, for dendritic dipeptides composed of enantiopure Tyr and racemized Ala, (4-3,4-3,5)12G2-CH$_2$-Boc-DL-Tyr-D-Ala-OMe and (4-3,4-3,5)12G2-CH$_2$-Boc-DL-Tyr-L-Ala-OMe, a T_e of 19 °C and an h_e of -26 kcal/mol were observed (Figure 9f). In both cases, the temperature of the transition from nucleation to elongation and the molar enthalpy of monomer addition were lower than expected for a 50/50 blend of homochiral and heterochiral dendritic dipeptides, suggesting that both homochiral and heterochiral dendritic

dipeptides will coassemble into single columns during the solution-phase supramolecular polymerization.

Further evidence for the coassembly of all stereoisomeric dendritic dipeptites into a single-column is provided by the self-assembly and self-organization of singly racemized dendritic dipeptides in the solid state. XRD analysis provides no indication of dissimilar supramolecular objects co-organized to form a superlattice. All of the partially racemized dendritic dipeptides self-organize into Φ_h lattices composed of columns with similar pore sizes (13.4–13.8 Å), but differing configurations of the dendritic dipeptides (Figure 8). Dendritic dipeptides with enantiopure Tyr but racemic Ala arrange into helical columns (Figure 8, top), whereas dendritic dipeptides with racemic Tyr but enantiopure Ala arrange into less ordered columns without demonstrable helicity over extended length scale (Figure 8, bottom). Interestingly, the racemization of either the Tyr or the Ala residue eliminates the effect of annealing on dendritic dipeptides in the bulk state (Figure 10 and Table 1). Both dendritic dipeptides racemized at Tyr or Ala exhibit $T_{\Phi-I}$ at 94 °C with associated transition enthalpy changes of 5.3 and 5.9 kcal/mol, respectively. Annealing at 80 °C for 60–180 min did not result in the emergence of a higher temperature phase or a
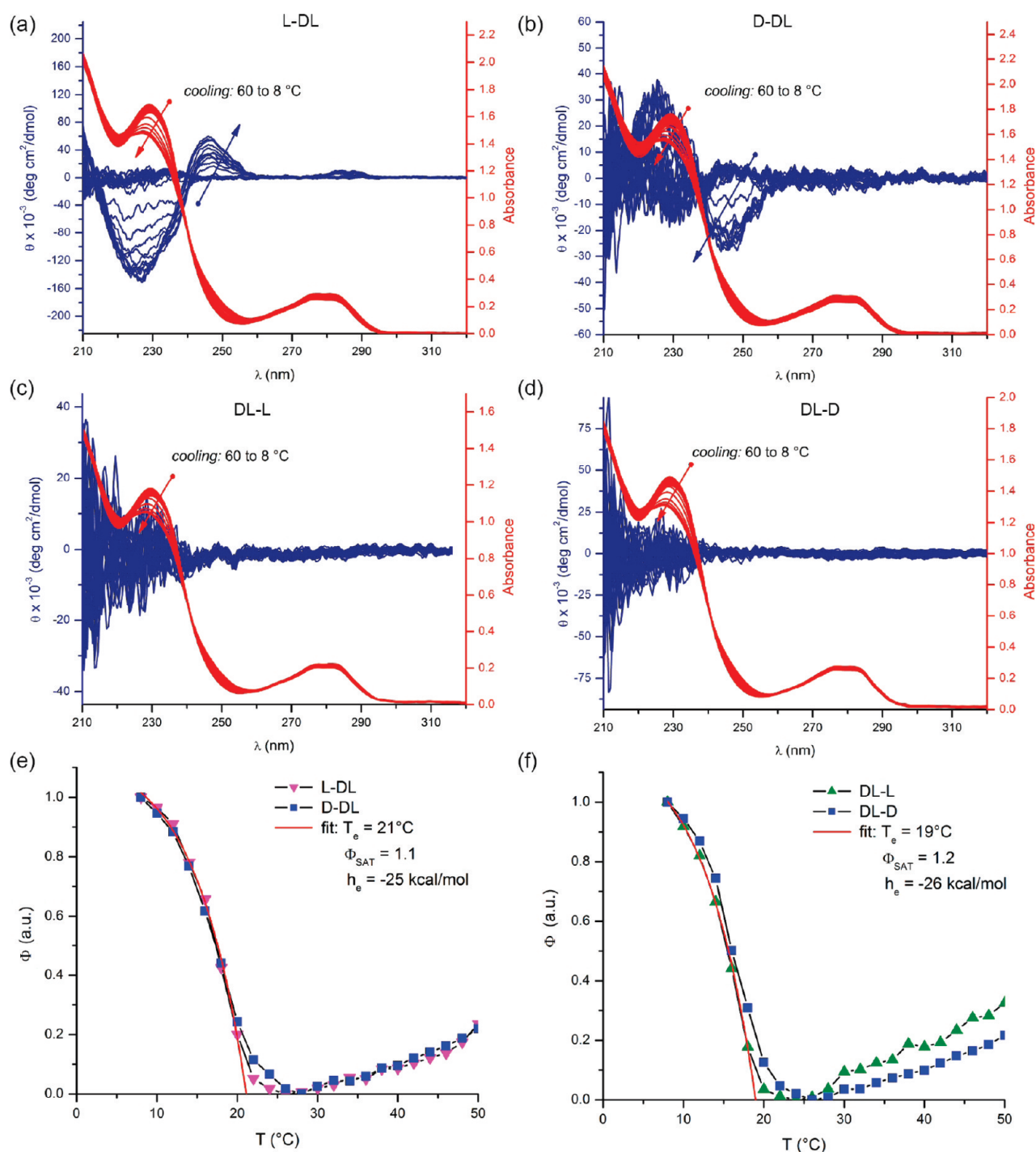
Figure 9. CD (blue) and UV−vis (red) of dendritic dipeptides with racemized Ala (a,b) or racemized Tyr (c,d) (1.6×10^{-4} M in cyclohexane). Degree of aggregation as a function of temperature for dendritic dipeptides containing racemic Ala (e) or racemic Tyr (f) calculated from UV−vis spectra.

significant increase in the enthalpy change of isotropization corresponding to an intracolumnar crystallization. Likewise, WAXS of the oriented fibers of the singly racemized dendritic dipeptides showed little change following the annealing process, indicating no major amplification of intracolumnar order (Figure 11).

Dendritic Dipeptides Composed of Racemized Tyr and Ala. The dendritic dipeptide (4-3,4-3,5)12G2-CH$_2$-Boc-DL-Tyr-DL-Ala-OMe containing racemic Tyr and racemic Ala was

prepared. As described in Figure 2, this dendritic dipeptide is in fact a 25:25:25:25 mixture of enantiomeric and diastereomeric pairs of all of the stereochemical permutations of the dendritic dipeptides:
(4-3,4-3,5)12G2-CH$_2$-Boc-D-Tyr-D-Ala-OMe, (4-3,4-3,5)12G2-CH$_2$-Boc-D-Tyr-L-Ala-OMe, (4-3,4-3,5)12G2-CH$_2$-Boc-L-Tyr-D-Ala-OMe, and (4-3,4-3,5)12G2-CH$_2$-Boc-L-Tyr-L-Ala-OMe. Consequently, the solution -phase supramolecular polymerization of the dendritic dipeptides could proceed in one of three
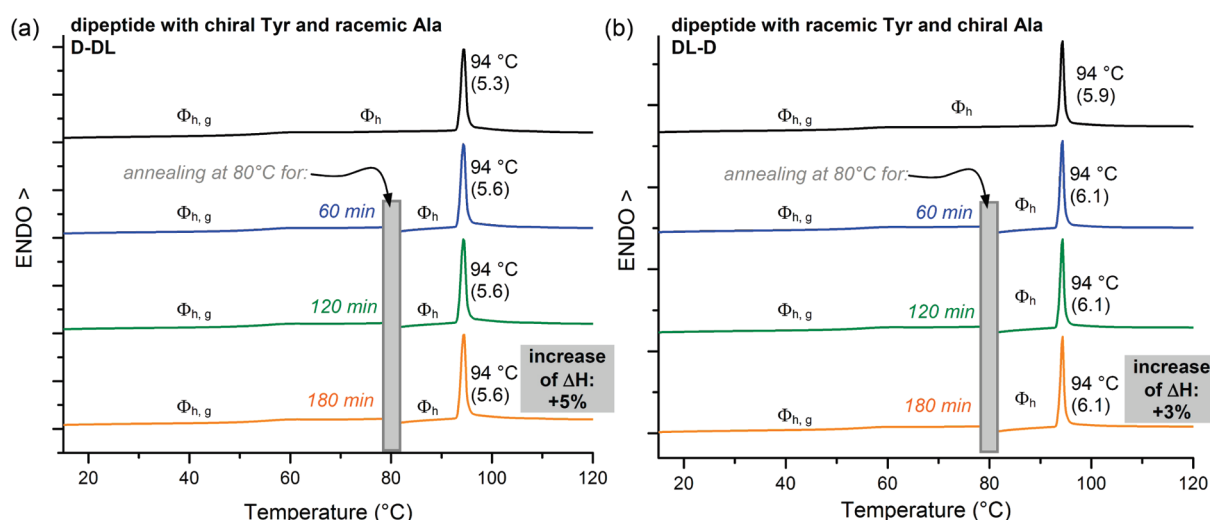
Figure 10. DSC traces upon heating of (4-3,4-3,5)12G2-CH$_2$-Boc-X-Tyr-Y-AlaOMe containing racemized Ala (D–DL) (a) or racemized Tyr (DL–D) (b) with various annealing times prior to isotropization. The associated enthalpy changes are indicated in parentheses (kcal/mol).

possible fashions: (a) into four enantiomerically and diastereomerically pure columns, (b) into 2−4 distinct columns composed of mixed diastereomers, or (c) coassembly of all four dendritic dipeptides into a single column (Figure 12).

For the dendritic dipeptides composed of a single racemic amino acid, the discrimination between the various modes of self-assembly can be made through the analysis of the temperature dependence on the degree of supramolecular polymerization. CD−UV/vis spectroscopy reveals that, as expected, the completely racemized dendritic dipeptide shows no net ellipticity (Figure 13a). For a mixture of all four enantiomerically and diastereomerically pure columns, a molar enthalpy of monomer addition of −30 to 35 kcal/mol is expected, while a mixture of 2−4 distinct columns composed of diastereomeric pairs is expected to result in a molar enthalpy of monomer addition of approximately −25 kcal/mol. Application of the model for helical cooperative self-assembly to the UV/vis spectra of the temperature-dependent solution-phase supramolecular polymerization of the completely racemized dendritic dipeptide provided a molar enthalpy of monomer addition of −19 kcal/mol (Figure 13b). This low molar enthalpy of monomer addition suggests the exclusion of all models of self-assembly except for self-assembly into a single mixed column. The mixed column forms because the self-assembly process is mediated by the dendritic part of the dendritic dipeptide. Once the column is generated, its intracolumnar order starts to form and is stabilized by H-bonding that is determined by the stereochemistry of the dipeptide. This mechanism is similar to the hydrophobic effect that mediates the folding of proteins. Once the folding occurs, its structure is stabilized via H-bonding.

The assertion of a single mixed column is supported in the solid state by XRD analysis suggesting a Φ_h lattice self-organized from a single supramolecular object, exhibiting a somewhat smaller pore diameter of 12.8 Å (Figure 12). As with the partially racemized dendritic dipeptides, the doubly racemized dendritic dipeptide does not exhibit significant enhancement of the isotropization enthalpy upon annealing (Figure 14 and Table 1). Likewise, no evidence of increased intracolumnar order was observed via XRD analysis after the annealing period.
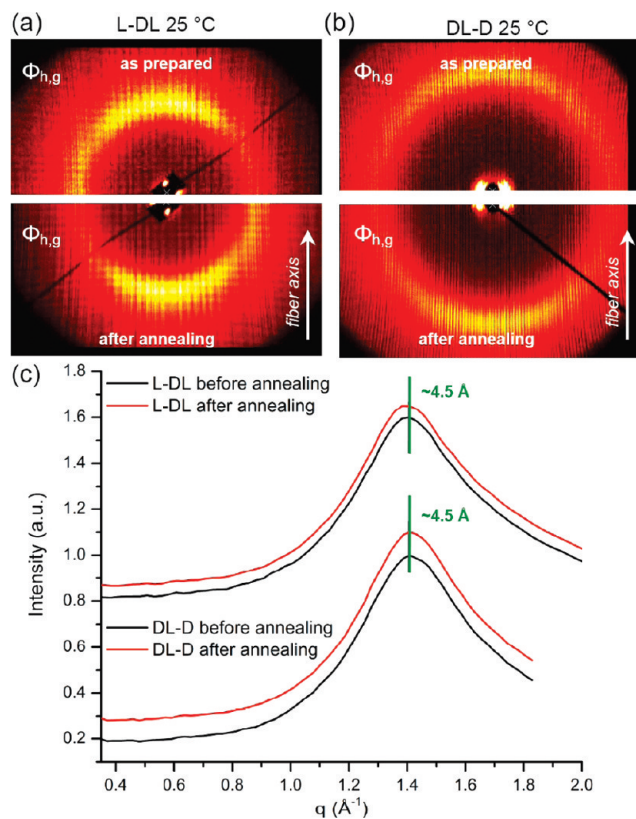

Figure 11. WAXS patterns collected from the oriented fibers of the dendritic dipeptide (4-3,4-3,5)12G2-CH$_2$-Boc-X-Tyr-Y-Ala-OMe, where X and Y are indicated (a,b). Meridional plots of the corresponding XRD patterns from (a) and (b) indicating that after annealing the dendritic dipeptides with either Tyr or Ala peptide racemized did not change their $\Phi_{h,g}$ phases (c).

Dendritic Dipeptides with Racemized Tyrosine and Chiral Alkyl Groups on the Periphery. It was shown in the previous sections that the fully racemized dendritic dipeptides self-assembled with lower enthalpy of monomer addition in the
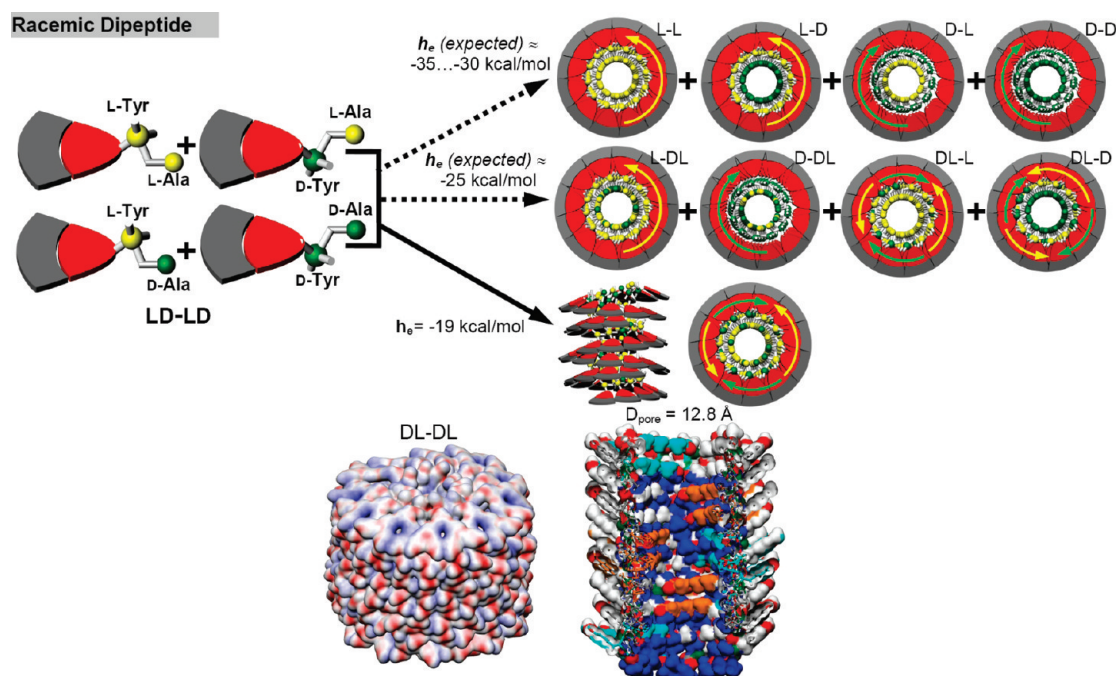
Figure 12. Self-assembly of racemic dendritic dipeptides into porous supramolecular columns via a helical cooperative growth. Schematic and analysis of self-assembly via supramolecular polymerization in solution and the corresponding side-view and cross-section of the supramolecular porous columns determined from XRD analysis in solid state. The color code of the dipeptides used in the cross-section of the porous supramolecular columns is explained in Figure 1b.
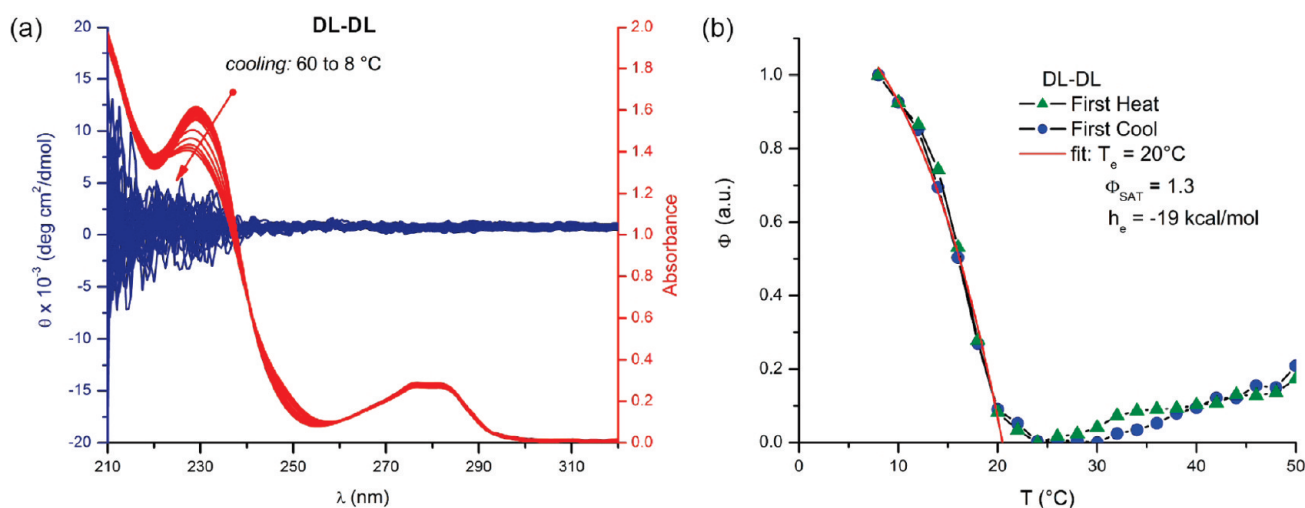

Figure 13. CD (blue) and UV−vis (red) of racemic dendritic dipeptides (a) $(1.6 \times 10^{-4}$ M in cyclohexane). Degree of aggregation as a function of temperature for racemic dendritic dipeptides (b).

supramolecular polymerization process and did not exhibit intracolumnar order in the solid state. This was the result of coassembly of all stereoisomers into mixed columns that did not express any helicity. The higher enthalpies and greater degree-of-order associated with the supramolecular polymerization of homochiral and to a lesser extent heterochiral and partially racemized dendritic dipeptides hint at a mechanism of amplification and selection of enantiomerically and diastereomerically enriched oligopeptide-containing systems. However, aside from statistical spontaneous deracemization,[53,54] these results do not offer a pathway by which the helical handedness of an otherwise racemic system could be selected.

One strategy to achieve the selection of the helix-sense would be to place a chiral unit at the periphery of dendritic dipeptide in the form of a chiral alkyl tail. As a first test of this approach, a chiral-tailed analogue of the fully racemized dendritic dipeptide was prepared using (S)-3,7-dimethyloctyl (dm8*) periphery units. This dendritic dipeptide $(4\text{-}3,4\text{-}3,5)\text{dm8*G2-CH}_2\text{-Boc-}$ DL-Tyr-DL-Ala-OMe was prepared but did not exhibit helical cooperative self-assembly. The presence of the branched tail likely reduced the temperature of nucleation below what could be observed in cyclohexane solution experiments. Two analogous dendritic dipetides with stereocenters in their alkyl periphery groups were prepared, $(6 \text{ Np-}3,4\text{-}3,5)\text{dm8*G2-CH}_2\text{-Boc-}$DL-

Tyr-DL-Ala-OMe and (6 Np-3,4-3,5)dm8*G2-CH2-Boc-DL-Tyr-L-Ala-OMe (Scheme 2), where the 4-substituted benzyl periphery unit was replaced with a 6-naphthyl periphery. The presence of the naphthyl groups[2f,33g,33h] was expected to increase the temperature of the nucleation to elongation transition in solution. Rewardingly, both the naphthyl-containing dendritic dipeptide
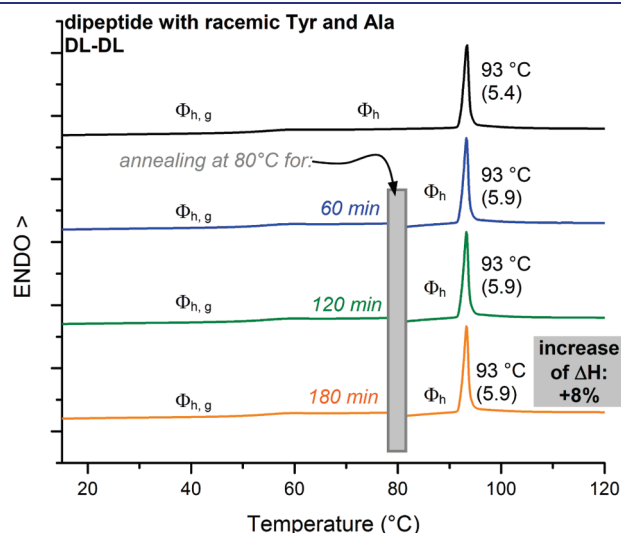
with racemized tyrosine and enantipure alanine, (6 Np-3,4-3,5)dm8*G2-CH2-Boc-DL-Tyr-L-Ala-OMe, and the naphthyl-containing dendritic dipeptide with fully racemized dendritic dipeptides exhibited a selection of helical handeness (Figure 15a, b) and helical cooperative self-assembly (Figure 15c,d). Furthermore, the temperature at which nucleation transitions into elongation and the enthalpy of supramolecular polymerization process are similar but slightly higher for the dendritic dipeptide containing racemized tyrosine but enantiopure alanine than for the dendron with a fully racemic dipeptide. These results indicate that the selection of helical handedness can occurs from either the periphery of the alkyl groups or the apex-dipeptide and that all stereoisomers of the dipeptide can be accommodated in the same helical column. Furthermore, it appears that the presence of a single enantiopure stereocenter in the dipeptide can be reinforced by the external chiral selection resulting in modest increase in the elongation transition temperature and enthalpy of monomer addition.

Perspectives on the Self-Assembly Mechanism. Application of temperature-dependent CD/UV−vis spectroscopy, modeling of the supramolecular structures resulting from the supramolecular polymerization in solution, and the examination of the self-organization and enhancement of intracolumnar order through annealing in solid state through DSC and XRD analysis to all stereochemical permutations of the dendritic dipeptide (4-3,4-3,5)12G2-Boc-X-Tyr-Y-Ala-OMe suggested a mechanism for the self-assembly of dendritic dipeptides. It is evident that these dendritic dipeptides self-assemble in solution through a process of helical cooperative supramolecular polymerization.
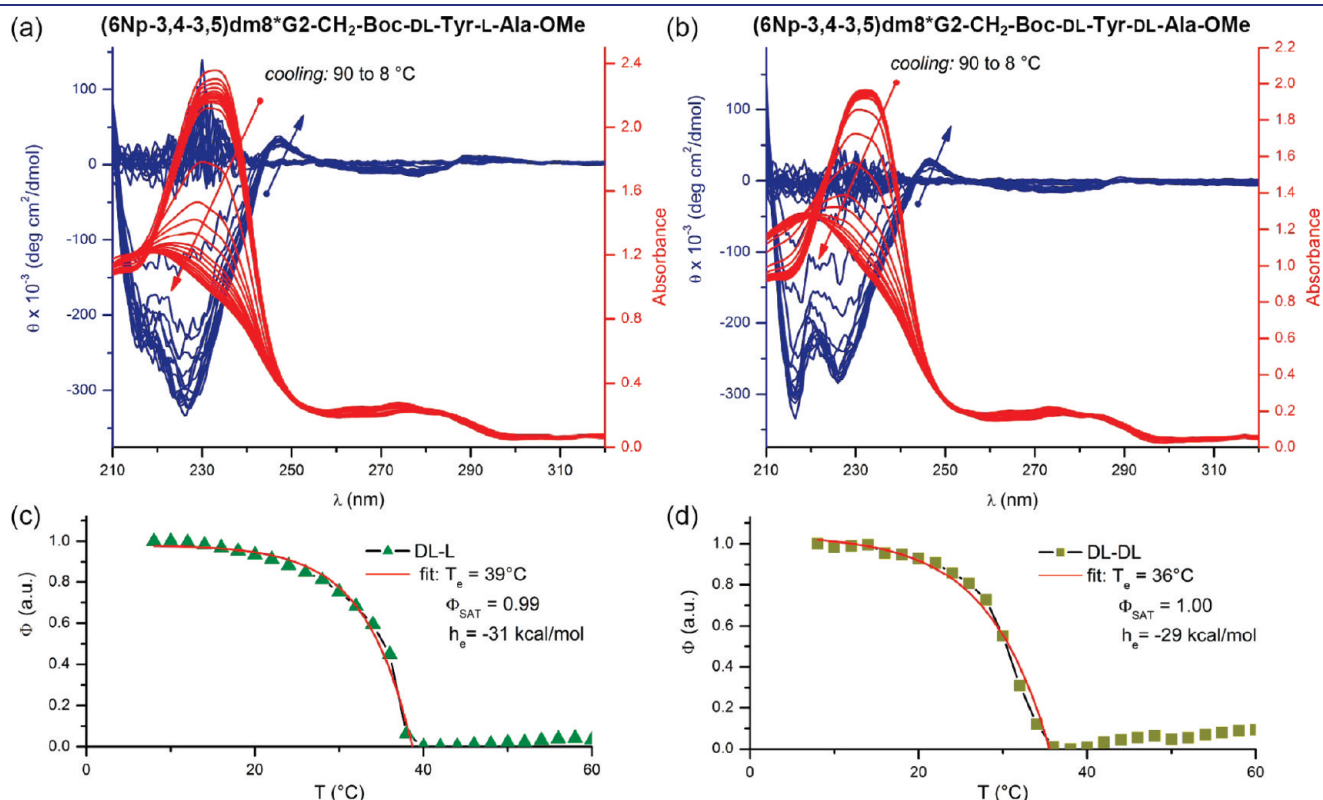

Figure 14. DSC traces upon heating of (4-3,4-3,5)12G2-CH2-Boc-DL-Tyr-DL-Ala-OMe with various annealing times prior to isotropization. The asssociated enthalpy changes are indicated in parentheses (kcal/mol).

Figure 15. CD (blue) and UV−vis (red) of napthyl-based dendritic dipeptides with chiral alkyl periphery groups, and a dipeptide containing racemic Tyr, (6 Np-3,4-3,5)dm8*G2-CH2-Boc-DL-Tyr-L-Ala-OMe, (a) or a fully racemic dipeptide, (6 Np-3,4-3,5)dm8*G2-CH2-Boc-DL-Tyr-DL-Ala-OMe, (b) (1.6 × 10⁻⁴ M in cyclohexanes). Degree of aggregation as a function of temperature for (6 Np-3,4-3,5)dm8*G2-CH2-Boc-DL-Tyr-L-Ala-OMe (c) and (6 Np-3,4-3,5)dm8*G2-CH2-Boc-DL-Tyr-DL-Ala-OMe (d).

5147

dx.doi.org/10.1021/ja200280h |J. Am. Chem. Soc. 2011, 133, 5135–5151

Table 2. Thermodynamic Data Calculated from the Fits of the UV Data Collected in Cyclohexane for (4-3,4-3,5)12G2-CH₂-Boc-X-Tyr-Y-Ala-OMe and from the DSC Data Collected with 10 °C/min after Annealing

dipeptide stereochemistry X—Y =	T_e (°C) [a,b,c]	T_m (°C) [a,b,c]	h_e (kcal/mol) [a,b,c]	T_{iso} (°C) [d]	ΔH (kcal/mol) [d]
L–L, D–D	24 ± 1 $[28 \pm 1]^e$	21 ± 1 $[24 \pm 1]^e$	-35 ± 3	105	13.3 ± 0.4
L–D, D–L	25 ± 1 $[28 \pm 1]^e$	21 ± 1 $[24 \pm 1]^e$	-30 ± 3	100	10.2 ± 0.4
L–DL, D–DL	21 ± 1	18 ± 1	-25 ± 3	94	5.6 ± 0.3
DL–L, DL–D	19 ± 1	16 ± 1	-26 ± 3	94	6.1 ± 0.3
DL–DL	20 ± 1	16 ± 1	-19 ± 3	93	5.9 ± 0.3

[a,b,c] T_e, T_m, and h_e calculated from the fit of the temperature dependence of the UV maxima from 226 nm using eq 1. [d] Isotropization transition temperature T_{iso} and associated enthalpy change ΔH measured by DSC after annealing in the Φ_h phase (Table 2). [e] For the homochiral and heterochiral dendritic dipeptides, a small hysteresis of ~4 °C was observed between heating and cooling data; the values in the square brackets were calculated from the fits of the UV data collected upon heating. Note: A possible hysteresis of ~1 °C was observed for all the racemized dendritic dipeptides, but the difference between heating and cooling cycles was comparable with the experimental error.

For enantio- and diasteriomerically pure dendritic dipeptides, the stereochemistry of the Tyr residue dictates the handedness of the supramolecular helical column, while the Ala residue allosterically regulates the structure of the column and the thermodynamics of the self-assembly process (Table 2). Homochiral dendritic dipeptides self-assemble with a higher molar enthalpy of monomer addition than heterochiral dendritic dipeptides. Therefore, it seems that the process of elongation/polymerization is more favorable for the homochiral stereoisomer. DSC and XRD analysis suggests that this process may be similar to the self-assembly and self-organization process in the solid state. DSC and XRD analysis show enhanced intracolumnar ordering and an increase in isotropization enthalpy change after annealing prior to $T_{\Phi-I}$. Because the supramolecular polymerization of homochiral dendritic dipeptides was enthalpically more favorable than that of heterochiral dendritic dipeptides, it is expected that homochiral dendritic dipeptides will form aggregates with higher degree of polymerization. Not only do we expect longer aggregates for the homochiral dendritic dipeptides, but it was also observed that there was more significant intracolumnar ordering following annealing to form a Φ_h^k phase (Figures 6a and 7a,c). This effect upon annealing was less dramatic for the heterochiral dendritic dipeptide, indicating a less pronounced intracolumnar order or crystallization (Figures 6b and 7b,c).

Helical selection was still possible when the Ala residue was racemized, but not if the Tyr residue or both residues were racemized. Whenever one or more of the residues was racemized, a continual decrease in the enthalpy of monomer addition was observed (Figure 16a), indicating that the different stereoisomers in the racemized mixture coassemble into a single column, diminishing the cooperativity and the degree of order within the columns. The mixing of stereoisomers into a single column and the resulting decrease in order was evidenced in XRD analysis. The increase in intracolumnar order upon annealing for homochiral and heterochiral dendritic dipeptides was absent in the case of partially and completely racemized dendritic dipeptides. Interestingly, hysteresis in the CD−UV/vis spectra between heating and cooling cycles was observed (Figure 16b, Supporting Information Figures SF2−5) for enantiopure dendritic dipeptides. However, this hysteresis was absent when one or both of the amino acids were racemized (Figure 16c). Hysteresis in cooperative supramolecular polymerization has been attributed to a kinetic barrier toward nucleation.[55] In some cases, such hysteresis can distinguish between homogoenous nucleation and heterogeneous nucleations, wherein nucleation is triggered by a seed particle, defect, or impurity.[55] It is possible
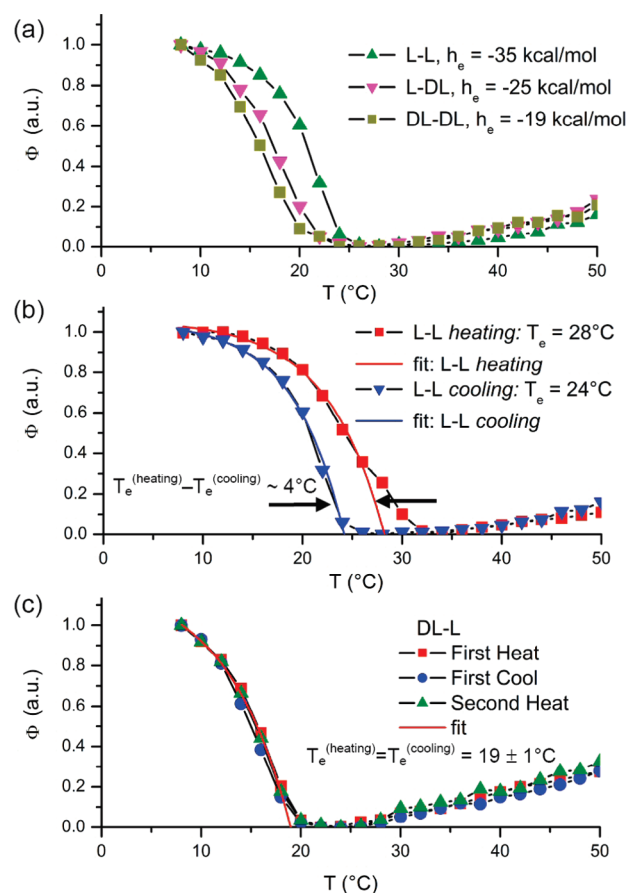

Figure 16. Degree of aggregation as a function of temperature calculated from the UV−vis: comparison between homochiral ((4-3,4-3,5)12G2-CH₂-Boc-L-Tyr-L-Ala-OMe) and partially ((4-3,4-3,5)12G2-CH₂-Boc-L-Tyr-DL-Ala-OMe) and fully ((4-3,4-3,5)12G2-CH₂-Boc-DL-Tyr-DL-Ala-OMe) racemized dendritic dipeptides (a), hysteresis between assembly and disassembly present in chiral dipeptides (b), and absent in the racemic Tyr or Ala (c).

that in the case of dendritic dipeptides containing one or more racemized amino acids, the dendritic dipeptide with mismatched stereochemistry can serve as a defect or "as impurity" in the presence of the other dendritic dipeptide and acts as a seed to initiate the heterogeneous nucleation.

To further elucidate the effect of incorporating dendritic dipeptides of mismatched chirality into a single column, a
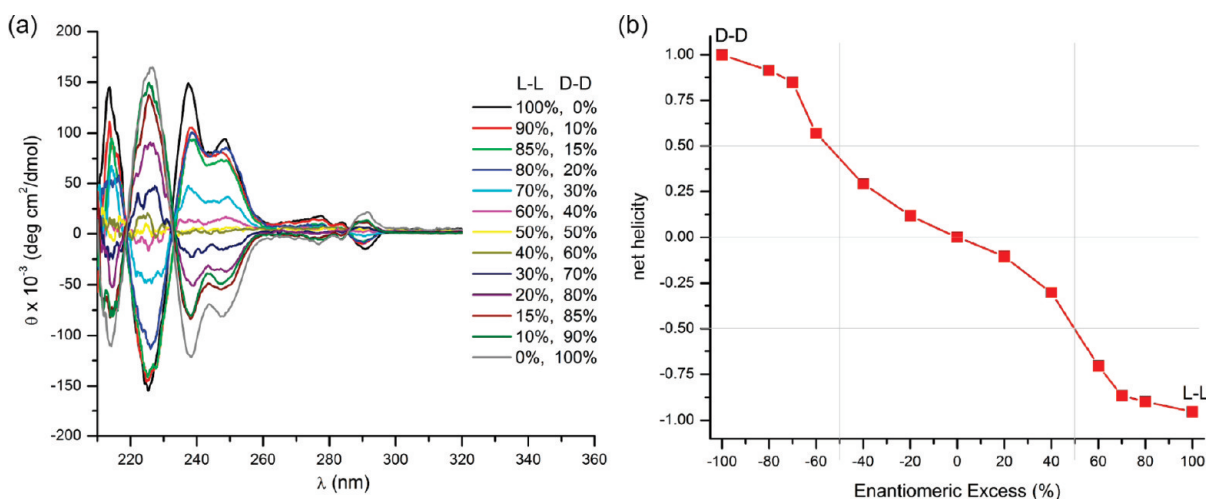
Figure 17. CD spectra collected from mixtures of L–L and D–D at 10 °C in cyclohexane (1.6×10^{-4} M) (a) and net helicity dependence (majority rule) of the enantiomeric excess (b).

majority-rules[56] experiment was performed (Figure 17). In the absence of majority-rules behavior, net helicity will increase linearly with enantiomeric excess. In typical majority-rules phenomena, net helicity will increase nonlinearly, outpacing the enantiomeric excess. The extent of majority rules is generally governed by the balance between monomer mismatch penalty (MMP), the cost of placing the incorrect stereoisomer in a suprastructure of the opposite handedness, and the helix reversal penalty (HRP), the energetic cost of inverting the helicity of a column. Mixtures of LL and DD dendritic dipeptides were prepared, and their CD spectra were measured as a function of composition (Figure 17). Here, the relationship between enantiomeric excess and net helicity is complex: 100% net helicity is only observed for 100% ee and falls off rapidly until 50% ee, where the net helicity decreases more slowly.

Although first observed in poly(isocyanates),[56] the theory developed for the analysis of majority-rules phenomena in supramolecular systems is based on discotic molecules, where a single molecule forms a stratum of the column.[51] The supramolecular polymerization of dendritic dipeptides represents an entirely different class of supramolecular polymer that more closely resembles the capsid suprastructure of TMV,[24,25] wherein each molecular monomer must contort its own preferred conformation to form a fraction of the stratum, than the columnar assemblies generated from discotic molecules. Here, not only can the dendritic monomer adapt its conformation to facilitate incorporation into a mismatched column, but as the concentration of minority monomer changes the entire structure of the columnar stratum can change producing an entirely different structure. The complex behavior found in the majority-rules experiment highlights the two distinct modes of self-assembly. For the enantiopure homochiral dendritic dipeptides LL and DD, highly enthalpically favorable helical cooperative self-assembly is observed. In this domain, the minority dendritic dipeptides with mismatched handedness begin to disrupt the long-range helical order (Supporting Information Figures SF1 and SF6). As the enantiomeric excess decreases, the columnar stratum begins to lose its helicity and the mechanism for the amplification and expression of chirality of majority dendritic dipeptides.

Surprisingly, CD/UV analysis in solution and XRD and DSC analysis in the solid state revealed no spontaneous

deracemization[53,54] for dendrons built from dipeptides containing one or more racemic α-amino acids. Analysis in the solid state demonstrated that the kinetics of intracolumnar crystallization was slow and decreased with diminished stereochemical purity. Therefore, it is evident that the dendritic part of the supramolecular column dominates the self-organization process, while the transfer of chirality from the dipeptidic apexes was slow, being observed only after annealing. Therefore, these results provide a possible explanation for the absence of spontaneous deracemization demonstrated by the CD/UV–vis experiments, which can only occur if the self-assembly is driven by the dipeptide. It is most probable that in solution, as suggested by the majority rules experiments, once the supramolecular assemblies are formed, the rate of exchange is very slow, due to the dominant role of the dendritic part.

■ CONCLUSIONS

In nature, homochirality and heterochirality is evident in a more grandious scale. Biological systems have evolved to produce single enantiomers of most classes of building blocks (e.g., amino acids, carbohydrates, nucleotides). Biological macromolecules prepared from these enantiopure building blocks are, therefore, typically entirely homochiral, composed of lengthy sequences of perfectly repeated stereochemistry. The consequences of stereopurity in the natural world are both marvelous and easily understood. Life could have also evolved as the mirror image of its contemporary form, but this Article demonstrates that a racemic or heterochiral world would bear no resemblence to the one in which we inhabit (e.g., the structural motifs of proteins are not stable for heterochiral arrangements of aminoacids). However, the origin of that chirality from the prebiotic mileu is more elusive and ultimately very challenging to prove. Nevertheless, few would disagree that the path toward biological homochirality must have involved the processes of both spontaneous deracemization and chiral amplification.[57]

It is now apparent that in the supramolecular polymerization of dendritic dipeptides, there is a thermodynamic preference for homochiral dipeptides over heterochiral or racemized dipeptides. The thermodynamic favorability of supramolecular polymerization and the long-range helical order that provides the

emergent function of the supramolecular porous columns is diminished by heterochirality and destroyed by racemization. Therefore, these dendritic dipeptides serve as a primitive model for the amplification of homochirality and its role to the origins of structure and function in nature, but also can elucidate the role of chirality on the function in biomolecular materials. Future work will explore the longer-range amplification of homochirality beyond dipeptides and the effect of external chiral influence on the spontaneous desymmetrization of racemic dendritic dipeptides.

■ ASSOCIATED CONTENT

ⓈSupporting Information. Experimental procedures with complete spectral analysis and complete refs 34b and 54e. This material is available free of charge via the Internet at http://pubs.acs.org.

■ AUTHOR INFORMATION

Corresponding Author
percec@sas.upenn.edu

■ ACKNOWLEDGMENT

■ REFERENCES

(1) *Supramolecular Polymers*; Ciferri, A., Ed.; Marcel Dekker: New York, 2000.

(2) (a) Sijbesma, R. P.; Meijer, E. W. *Curr. Opin. Colloid Interface Sci.* **1999**, *4*, 24–32. (b) Moore, J. S. *Curr. Opin. Colloid Interface Sci.* **1999**, *4*, 108–116. (c) Brunsveld, L.; Folmer, B. J. B.; Meijer, E. W.; Sijbesma, R. P. *Chem. Rev.* **2001**, *101*, 4071–4097. Sherrington, D. C.; Taskinen, K. A. *Chem. Soc. Rev.* **2001**, *30*, 89–93. (d) Lehn, J.-M. *Polym. Int.* **2002**, *51*, 825–839. (e) Percec, V.; Imam, M. R.; Bera, T. K.; Balagurusamy, V. S. K.; Peterca, M.; Heiney, P. A. *Angew. Chem., Int. Ed.* **2005**, *44*, 4739–4745. (f) Percec, V.; Johansson, G.; Ungar, G.; Zhou, J. P. *J. Am. Chem. Soc.* **1996**, *118*, 9855–9866. (g) Rosen, B. M.; Wilson, C. J.; Wilson, D. A.; Peterca, M.; Imam, M. R.; Percec, V. *Chem. Rev.* **2009**, *109*, 6275–6540.

(3) (a) Lehn, J.-M. *Angew. Chem. Int. Ed., Engl.* **1990**, *29*, 1304–1319. (b) Lehn, J.-M. *Supramolecular Chemistry − Concepts and Perspectives*; Wiley-VCH: Weinheim, 1995.

(4) Ciferri, A. *Prog. Polym. Sci.* **1995**, *20*, 1081–1120.

(5) Ciferri, A. *J. Macromol. Sci., Part C: Polym. Rev.* **2003**, *C43*, 271–322.

(6) De Greef, T. F. A.; Smulders, M. M. J.; Wolffs, M.; Schenning, A. P. H. J.; Sijbesma, R. P.; Meijer, E. W. *Chem. Rev.* **2009**, *109*, 5687–5754.

(7) Fouquey, C.; Lehn, J.-M.; Levelut, A.-M. *Adv. Mater.* **1990**, *2*, 254–257.

(8) Park, T.; Zimmerman, S. C. *J. Am. Chem. Soc.* **2006**, *128*, 13986–13987.

(9) (a) Kihara, H.; Kato, T.; Uryu, T.; Frechet, J. M. J. *Chem. Mater.* **1996**, *8*, 961–968. (b) Ungar, G.; Abramic, D. I.; Percec, V.; Heck, J. A. *Liq. Cryst.* **1996**, *21*, 73–86.

(10) (a) Percec, V.; Heck, J.; Tomazos, D.; Falkenberg, F.; Blackwell, H.; Ungar, G. *J. Chem. Soc., Perkins Trans. 1* **1993**, 2799–2811. (b) Beijer, F. H.; Sijbesma, R. P.; Kooijman, H.; Spek, A. L.; Meijer, E. W. *J. Am. Chem. Soc.* **1998**, *120*, 6761–6769.

(11) Palmans, A. R. A.; Vekemans, J. A. J. M.; Havinga, E. E.; Meijer, E. W. *Angew. Chem., Int. Ed. Engl.* **1997**, *36*, 2648–2651.

(12) van Hamerern, R.; Schön, P.; van Buul, A. M.; Hoogboom, J.; Lazarenko, S. V.; Gerritsen, J. W.; Engelkamp, H.; Christianen, P. C. M.; Heus, H. A.; Maan, J. C.; Rasing, T.; Speller, S.; Rowan, A. E.; Elemans, J. A. A. W.; Nolte, R. J. M. *Science* **2006**, *314*, 1433–1436.

(13) Zhao, D.; Moore, J. S. *Org. Biomol. Chem.* **2003**, *1*, 3471–3491.

(14) Kastler, M.; Pusla, W.; Wassefallen, D.; Pakula, T.; Müllen, K. *J. Am. Chem. Soc.* **2005**, *127*, 4286–4296.

(15) (a) Würthner, F.; Thalacker, C.; Diele, S.; Tschierske, C. *Chem.-Eur. J.* **2001**, *7*, 2245–2253. (b) Percec, V.; Glodde, M.; Bera, T. K.; Miura, Y.; Shiyanovskaya, I.; Singer, K. D.; Balagurusamy, V. S. K.; Heiney, P. A.; Schnell, I.; Rapp, A.; Spiess, H.-W.; Hudson, S. D.; Huan, H. *Nature* **2002**, *419*, 384–387.

(16) Hill, J. P.; Jin, W.; Kosaka, A.; Fukushima, T.; Ichihara, H.; Shimomura, T.; Ito, K.; Hashizume, T.; Ishii, N.; Aida, T. *Science* **2004**, *304*, 1481–1483.

(17) (a) Percec, V.; Heck, J. A.; Tamazos, D.; Ungar, G. *J. Chem. Soc., Perkins Trans. 2* **1993**, 2381–2388. (b) Percec, V.; Johansson, G.; Heck, J.; Ungar, G.; Batty, S. V. *J. Chem. Soc., Perkins Trans. 1* **1993**, 1411–1420. (c) Percec, V.; Heck, J.; Johansson, G.; Tomazos, D.; Kawasumi, M.; Chu, P.; Ungar, G. *J. Macromol. Sci., Part A: Pure Appl. Chem.* **1994**, *A31*, 1719–1758.

(18) Castellano, R. K.; Rudkevich, D. M.; Rebek, J., Jr. *Proc. Natl. Acad. Sci. U.S.A.* **1997**, *94*, 7132–7137.

(19) Ciferri, A. *Macromol. Rapid Commun.* **2002**, *23*, 511–529.

(20) Dudowicz, J.; Freed, K. F.; Douglas, J. F. *J. Chem. Phys.* **2003**, *119*, 12645–12666.

(21) Oosawa, F.; Kasai, M. *J. Mol. Biol.* **1962**, *4*, 10–21.

(22) Goldstein, R. F.; Stryer, L. *Biophys. J.* **1986**, *50*, 583–599.

(23) Van der Schoot, P. In *Supramolecular Polymers*, 2nd ed.; Ciferri, A., Ed.; Taylor & Francis: London, 2005.

(24) Klug, A. *Angew. Chem., Int. Ed. Engl.* **1983**, *22*, 565–582.

(25) Klug, A. *Philos. Trans. R. Soc. London, Ser. B* **1999**, *354*, 531–535.

(26) (a) Balagurusamy, V. S. K.; Ungar, G.; Percec, V.; Johansson, G. *J. Am. Chem. Soc.* **1997**, *119*, 1539–1555. (b) Percec, V.; Cho, W.-D.; Ungar, G.; Yeardley, D. J. P. *J. Am. Chem. Soc.* **2001**, *123*, 1302–1315. (c) Peterca, M.; Imam, M. R.; Ahn, C.-H.; Balagurusamy, V. S. K.; Wilson, D. A.; Rosen, B. M.; Percec, V. *J. Am. Chem. Soc.* **2011**, *133*, 2311–2328. (d) Peterca, M.; Percec, V. *Science* **2010**, *330*, 333–334.

(27) Yeardley, D. J. P.; Ungar, G.; Percec, V.; Holerca, M. N.; Johansson, G. *J. Am. Chem. Soc.* **2000**, *122*, 1684.

(28) Ungar, G.; Liu, Y.; Zeng, X.; Percec, V.; Cho, W.-D. *Science* **2003**, *299*, 1208–1211.

(29) Zeng, X.; Ungar, G.; Liu, Y.; Percec, V.; Dulcey, A. E.; Hobbs, J. K. *Nature* **2004**, *428*, 157–160.

(30) Percec, V.; Peterca, M.; Sienkowska, M. J.; Ilies, M. A.; Aqad, E.; Smidrkal, J.; Heiney, P. A. *J. Am. Chem. Soc.* **2006**, *128*, 3324–3334.

(31) (a) Percec, V.; Holerca, M. N.; Nummelin, S.; Morrison, J. J.; Glodde, M.; Smidrkal, J.; Peterca, M.; Rosen, B. M.; Uchida, S.; Balagurusamy, V. S. K.; Sienkowska, M. J.; Heiney, P. A. *Chem.-Eur. J.* **2006**, *12*, 6216–6241. (b) Percec, V.; Smidrkal, J.; Peterca, M.; Mitchell, C. M.; Nummelin, S.; Dulcey, A. E.; Sienkowska, M.; Heiney, P. A. *Chem.-Eur. J.* **2007**, *13*, 3989–4007.

(32) Percec, V.; Won, B. C.; Peterca, M.; Heiney, P. A. *J. Am. Chem. Soc.* **2007**, *129*, 11265–11278.

(33) (a) Percec, V.; Dulcey, A. E.; Balagurusamy, V. S. K.; Miura, Y.; Smidrkal, J.; Peterca, M.; Nummelin, S.; Edlund, Y.; Hudson, S. D.; Heiney, P. A.; Duan, H.; Maganov, S. N.; Vinogradov, S. A. *Nature* **2004**, *430*, 764–768. (b) Percec, V.; Dulcey, A. E.; Peterca, M.; Adelman, P.; Samant, R.; Balagurusamy, V. S. K.; Heiney, P. A. *J. Am. Chem. Soc.* **2007**, *129*, 5992–6002. (c) Percec, V.; Dulcey, A. E.; Peterca, M.; Ilies, M.; Miura, Y.; Edlund, Y.; Heiney, P. A. *Aust. J. Chem.* **2005**, *58*, 472–482. (d) Percec, V.; Dulcey, A. E.; Peterca, M.; Ilies, M.; Nummelin, S.; Sienkowska, M. J.; Heiney, P. A. *Proc. Natl. Acad. Sci. U.S.A.* **2006**, *103*, 2518–2523. (e) Percec, V.; Dulcey, A. E.; Peterca, M.; Ilies, M.; Ladislaw, J.; Rosen, B. M.; Edlund, U.; Heiney, P. A. *Angew. Chem., Int. Ed.* **2005**, *44*, 6516–6521. (f) Percec, V.; Dulcey, A. E.; Peterca, M.; Ilies,

M.; Sienkowska, M.; Heiney, P. A. *J. Am. Chem. Soc.* **2005**, *127*, 17902–17909. (g) Kaucher, M. S.; Peterca, M.; Dulcey, A. E.; Kim, A. J.; Vinogradov, S. A.; Hammer, D. A.; Heiney, P. A.; Percec, V. *J. Am. Chem. Soc.* **2007**, *129*, 11698–11699. (h) Kim, A. J.; Kaucher, M. S.; Davis, K. P.; Peterca, M.; Imam, M. R.; Christian, N. A.; Levine, D. A.; Bates, F. S.; Percec, V.; Hammer, D. A. *Adv. Funct. Mater.* **2009**, *19*, 2930–2936.

(34) (a) Percec, V.; Peterca, M.; Dulcey, A. E.; Imam, M. R.; Hudson, S. D.; Nummelin, S.; Adelman, P.; Heiney, P. A. *J. Am. Chem. Soc.* **2008**, *130*, 13079–13094. (b) Percec, V. *Science* **2010**, *328*, 1009–1014.

(35) Cochran, W.; Crick, F. H. C.; Vand, V. *Acta Crystallogr.* **1952**, *5*, 581–586.

(36) Peterca, M.; Percec, V.; Imam, M. R.; Leowanawat, P.; Morimitsu, K.; Heiney, P. A. *J. Am. Chem. Soc.* **2008**, *130*, 14840–14852.

(37) Peterca, M.; Percec, V.; Dulcey, A. E.; Nummelin, S.; Korey, S.; Ilies, M.; Heiney, P. A. *J. Am. Chem. Soc.* **2006**, *128*, 6712–6720.

(38) (a) Percec, V.; Aqad, E.; Peterca, M.; Imam, M. R.; Glodde, M.; Bera, T. K.; Miura, Y.; Balagurusamy, V. S. K.; Ewbank, P. C.; Würthner, F.; Heiney, P. A. *Chem.-Eur. J.* **2007**, *13*, 3330–3345. (b) Percec, V.; Glodde, M.; Peterca, M.; Rapp, A.; Schnell, I.; Spiess, H. W.; Bera, T. K.; Miura, Y.; Balagurusamy, V. S. K.; Aqad, E.; Heiney, P. A. *Chem.-Eur. J.* **2006**, *12*, 6298–6314.

(39) Percec, V.; Peterca, M.; Yurchenko, M. E.; Rudick, J. G.; Heiney, P. A. *Chem.-Eur. J.* **2007**, *14*, 909–918.

(40) (a) Percec, V.; Peterca, M.; Rudick, J. G.; Aqad, E.; Imam, M. R.; Heiney, P. A. *Chem.-Eur. J.* **2007**, *13*, 9572–9581. (b) Percec, V.; Rudick, J. G.; Peterca, M.; Heiney, P. A. *J. Am. Chem. Soc.* **2008**, *130*, 7503–7508. (c) Rudick, J. G.; Percec, V. *Acc. Chem. Res.* **2008**, *41*, 1641–1652.

(41) (a) *Asymmetric Synthesis and Applications of α-Amino Acids*; Soloshonok, V. A., Izawa, K., Eds.; ACS Symposium Series: Washington, DC, 2009; Vol. 1009. (b) O'Donnell, M. J. *Acc. Chem. Res.* **2004**, *37*, 506–517.

(42) Kronin, J. S.; Ginah, F. O.; Murray, A. R.; Copp, J. D. *Synth. Commun.* **1996**, *26*, 3491–3494.

(43) Peterca, M.; Imam, M. R.; Leowanawat, P.; Rosen, B. M.; Wilson, D. A.; Wilson, C. J.; Zeng, X.; Ungar, G.; Heiney, P. A.; Percec, V. *J. Am. Chem. Soc.* **2010**, *132*, 11288–11305.

(44) Percec, V. *Philos. Trans. R. Soc. London, Ser. A* **2006**, *364*, 2709–2719.

(45) Percec, V.; Heck, J.; Lee, M.; Ungar, G.; Alvarez-Castillo, A. *J. Mater. Chem.* **1992**, *2*, 1033–1039.

(46) Schenning, A. P. H. J.; Jonkheijm, P.; Peeters, E.; Meijer, E. W. *J. Am. Chem. Soc.* **2001**, *123*, 409–416.

(47) Jonkheijm, P.; van der Schoot, P.; Schenning, A. P. H. J.; Meijer, E. W. *Science* **2006**, *313*, 80–83.

(48) Percec, V.; Ungar, G.; Peterca, M. *Science* **2006**, *313*, 55–56.

(49) Smulders, M. M. J.; Schenning, A. P. H. J.; Meijer, E. W. *J. Am. Chem. Soc.* **2008**, *130*, 606–611.

(50) Green, M. M.; Garetz, B. A.; Munoz, B.; Chang, H. P.; Hoke, S.; Cooks, R. G. *J. Am. Chem. Soc.* **1996**, *117*, 4181–4182.

(51) (a) Jin, W.; Fukushima, T.; Niki, M.; Kosaka, A.; Ishii, N.; Aida, T. *Proc. Natl. Acad. Sci. U.S.A.* **2005**, *102*, 10801–10806. (b) van Gestel, J.; Palmans, A. R. A.; Titulaer, B.; Vekemans, J. A. J. M.; Meijer, E. W. *J. Am. Chem. Soc.* **2005**, *127*, 5490–5494.

(52) (a) van Gestel, J.; van der Schoot, P.; Michels, M. A. J. *Macromolecules* **2003**, *36*, 668–673. (b) Smulders, M. M. J.; Stals, P. J. M.; Mes, T.; Paffen, T. F. E.; Schenning, A. P. H. J.; Palmans, A. R. A.; Meijer, E. W. *J. Am. Chem. Soc.* **2010**, *132*, 620–626. (c) Smulders, M. M. J.; Nieuwhenheizen, M. M. L.; de Greef, T. F. A.; van der Schoot, P.; Schenning, A. P. H. J.; Meijer, E. W. *Chem.-Eur. J.* **2010**, *16*, 362–367.

(53) (a) Pasteur, L. *Ann. Chim. Phys.* **1848**, *24*, 442–459. (b) Fasel, R.; Parschau, M.; Ernst, K.-H. *Nature* **2006**, *439*, 449–452. (c) Takanishi, Y.; Takezoe, H.; Suzuki, Y.; Kobayashi, I.; Yajima, T.; Terada, M.; Mikami, K. *Angew. Chem., Int. Ed.* **1999**, *38*, 2354–2356. (d) Jeong, H. S.; Tanaka, S.; Yoon, D. K.; Choic, S.-W.; Kim, Y. H.; Kawauchi, S.; Araoka, F.; Takezoe, H.; Jung, H.-T. *J. Am. Chem. Soc.* **2009**, *131*, 15055–15060. (e) Nagayama, H.; Varshney, S. K.; Goto, M.; Araoka, F.; Ishikawa, K.;

Prasad, V.; Takezoe, H. *Angew. Chem., Int. Ed.* **2010**, *49*, 445–448. (f) Pérez-García, L.; Amabilino, D. B. *Chem. Soc. Rev.* **2002**, *31*, 342–356.

(54) (a) Walba, D. M.; Korblova, E.; Huang, C. C.; Shao, R. F.; Nakata, M.; Clark, N. A. *J. Am. Chem. Soc.* **2006**, *128*, 5318–5319. (b) Link, D. R.; Natale, G.; Shao, R.; Maclennan, J. E.; Clark, N. A.; Korblova, E.; Walba, D. M. *Science* **1997**, *278*, 1924–1927. (c) Walba, D. M.; Korblova, E.; Shao, R.; Maclennan, J. E.; Link, D. R.; Glaser, M. A.; Clark, N. A. *Science* **2000**, *288*, 2181–2184. (d) Hough, L. E.; Spannuth, M.; Nakata, M.; Coleman, D. A.; Jones, C. D.; Dantlgraber, G.; Tschierske, C.; Watanabe, J.; Korblova, E.; Walba, D. M.; Maclennan, J. E.; Glaser, M. A.; Clark, N. A. *Science* **2009**, *325*, 452–456. (e) Hough, L. E.; et al. *Science* **2009**, *325*, 456–460. (f) Shcherbina, M. A.; Zeng, X. B.; Tadjiev, T.; Ungar, G.; Eichhorn, S. H.; Phillips, K. E. S.; Katz, T. J. *Angew. Chem., Int. Ed.* **2009**, *48*, 7837–7840.

(55) Schulman, R.; Winfree, E. *Proc. Natl. Acad. Sci. U.S.A.* **2007**, *104*, 15236–15241.

(56) Green, M. M.; Garetz, B. A.; Munoz, B.; Chang, H. P.; Hoke, S.; Cooks, R. G. *J. Am. Chem. Soc.* **1995**, *117*, 4181–4182.

(57) Frank, P.; Bonner, W. A.; Zare, R. N. In *Chemistry for the 21st Century*; Keinan, E., Schechter, I., Eds.; Wiley-VCH: Weinheim, Germany, 2001; pp 175–208.

5151

dx.doi.org/10.1021/ja200280h |*J. Am. Chem. Soc.* 2011, 133, 5135–5151